The ESA Active Dosimeter (EAD) system onboard the International Space Station (ISS)

Ulrich Straube[a,*], **Thomas Berger**[b], **Matthias Dieckmann**[c]

[a] European Astronaut Centre (EAC), Space Medicine Team, Cologne, Germany
[b] German Aerospace Center (DLR), Institute of Aerospace Medicine, Cologne, Germany
[c] European Space Research and Technology Centre (ESTEC), Noordwijk, the Netherlands

Received 23 May 2022; accepted 7 March 2023

Abstract

Ionizing radiation in general and mixed fields of space radiation in particular pose a risk of serious harm to human health. The risk of such adverse effects increases with the duration of the mission, and for all missions outside the protective properties of the Earth's magnetic field and atmosphere. Accordingly, radiation protection is of central importance for all human spaceflight, which is recognized by all international space agencies. To date various systems, analyze and determine the exposure to ionizing radiation within the environment and to the crew onboard the International Space Station (ISS). In addition to this operational monitoring, experiments and technology demonstrations are carried out. This to further enhance systems capabilities, to prepare for exploratory missions, to the Deep Space Gateway and/or to enable for human presence at other celestial bodies. Subsequently the European Space Agency (ESA) decided early to support the development of an active personal dosimeter. Under the auspices of the European Space Research and Technology Center (ESTEC) together with the European Astronaut Center's (EAC) Medical Operations and Space Medicine (HRE-OM) team, a European industrial consortium was formed to develop, build, and test this system. To complete the ESA Active Dosimeter (EAD) Technology Demonstration in space, EAD components were delivered to ISS with the ESA's space missions 'iriss' and 'proxima' in 2015 and 2016. This marked Phase 1 (2015) and 2 (2016–2017) of the EAD Technology Demonstration to which focus is given in this publication. All EAD systems and their functionalities, the different radiation detector, their properties, and calibrations procedures are described. Emphasis is first on the "iriss" mission of September 2015, that provided a complete set of data for an entire space mission from launch to landing, for the first time. Data obtained during Phase 2 in 2016–2017 are discussed thereafter. Measurements with the active radiation detectors of the EAD system provided data of the absorbed dose, dose equivalent, quality factor as well as the various dose contributions during the crossings of the South Atlantic Anomaly (SAA) and/or resulting from galactic cosmic radiation (GCR). Results of the in-flight cross-calibrations among the internal sensors of the EAD systems are discussed and alternative usage of the EAD Mobile Units as area monitors at various different locations inside the ISS is described.

Keywords: International Space Station; Human Space Flight; Galactic Cosmic Radiation; South Atlantic Anomaly; Space Radiation Dosimetry; Radiation Protection; Solar Particle Events; Ionizing Radiation

1 Introduction

Tremendous changes have taken place since the proclamation of the space age, from unmanned rockets that could launch artificial celestial bodies like Sputnik to the first human presence in space by cosmonaut Yuri Gagarin. This was followed by the first space walks of astronauts and, as a preliminary crowning achievement, the first presence of humans on the surface of the Moon, now already 53 years ago, on July 20, 1969, during the Apollo program. Thanks to the construction of the ISS and more recently the Chinese Space Station (CSS), a permanent human presence in space has been achieved in recent decades. Today, spacefaring nations and the international human spaceflight community are focused on realizing missions beyond low Earth orbit (BLEO) as well as the promotion of the commercial access to space. There are strong calls in Europe and North America to return to the Moon and to make the necessary efforts to

* Corresponding author: Ulrich Straube, European Astronaut Centre (EAC), Space Medicine Team (HRE-OM), Cologne, Germany.
E-mail: ulrich.straube@esa.ext.int (U. Straube).

Z Med Phys **xxx** (2023) xxx–xxx
https://doi.org/10.1016/j.zemedi.2023.03.001
www.elsevier.com/locate/zemedi

provide a prolonged human presence on and below the lunar surface as well. The quest for missions into deep space and to explore Mars is becoming more and more concrete, sparking ideas for further scenarios and technologies that go beyond the conventional human spaceflight paradigm of the recent past. Commercial companies emerged with alternative concepts previously thought feasible only in the context of national and/or multinational programs. Altogether this could lead to the fact that in retrospect, one may speak of the dawn of a truly new space age for this and future generations.

Despite the great strides that human spaceflight has made, ionizing radiation remains on the list of concerns for crew health and is regularly cited in the context of the major health risks of spaceflight. However, as far as the authors are aware, there is no evidence that radiation exposure was ever the sole cause of crew performance degradation and/or mission success being compromised. Nevertheless, exposure to ionizing radiation in space is undoubtedly different in quality and quantity from any occupational exposure that may be routinely encountered on Earth. Radiation exposure in space must continue to be closely monitored and managed in accordance with radiation protection regulations and thus the ALARA (As Low As Reasonably Achievable) paradigm.

There are numerous hurdles, especially for human spaceflight BLEO. Future space exploration places high demands on spacecraft design that is based on the utilization of today's knowledge and technologies. To mention just one major practical consequence the reduced mass on board the spacecraft and thus at the destination. Missions to deep space may experience limited or complete loss of real-time communications more frequently than in low Earth orbit (LEO). Current radiation monitoring systems onboard the ISS and spacecraft built for missions BLEO provide independent monitoring capabilities also for ionizing radiation onboard. However, interruption of communications with the ground may prove detrimental to immediate decision making in extraordinary situations that may involve crew health problems and/or anomalies in the radiation environment.

As part of mandatory health surveillance for all ISS crew's personal dosimetry is still the gold standard. For ESA astronauts as for astronauts from ISS Partner Agencies, this is still performed by means of passive dosimeters of the individual (for ESA with the European Crew Personal Dosimeter, EuCPD) [1]. However, passive personal dosimetry for astronauts on extended long-term- and/or exploration-missions will not be sufficient. This is because such dosimetry typically provides its results only after the return to Earth and postprocessing. Hence, to address conditions identified and to provide a state-of-the-art system that enables meeting requirements in the future to determine the crew members exposure as mandatory part of the health surveillance, the development and design of an advanced dosimeter system was pursued. This resulted in the development of the first dosimetry systems taking advantage of multiple different active radiation detectors integrated into a compact system. A system that consists of a stationary unit as well as several mobile dosimeters and was accepted for testing within a human spaceflight mission onboard the ISS. Originally, the system was called European Crew Personal Active Dosimeter (EuCPAD) [2–3] during the phase of development. For its operational deployment aboard the ISS, the system then was renamed to ESA Active Dosimeter (EAD = ISS Operational Nomenclature (ISS OpNom)). Operations of the EAD system took place in the frame of an ESA Technology Demonstration (TechDemo). The system offered for the first-time advanced possibilities of measuring individual/personal dosimetry of a crew member in real time on board the ISS but also enabled the serving for stationary and mobile dosimetric measurements assessing the radiation environment within the different modules of the ISS. The EAD system provided advanced data reading-, display- and storage capabilities as well as means for autonomous data transmission to the ground plus options to control and operate from the earthbound ground stations. The goal of this article is to introduce the entire EAD system. This while putting focus on outlining and discussion of all information gained during ESA TechDemo onboard ISS, hence the measurements taken, the analyses executed, and the results obtained.

2 The EAD system

The EAD [2,3] system consists of the following subsystems: (a) the EAD-Personal Storage Device (EAD-PSD) (see Fig. 1), (b) the EAD-PSD data and power cable and (c) the five EAD-Mobile Units (EAD-MUs) (see Fig. 2).

The EAD-PSD (see front side in Fig. 1a) is equipped with a touchscreen interface for crew interaction as for visualization of their individual exposure on their EAD-MU, a data and a power connector, an ON/OFF switch for power and the so-called EAD-MU-reader-head.

In addition, the EAD-PSD houses two radiation detector systems. The first in-built radiation detector is the EAD-Tissue Equivalent Proportional Counter (EAD-TEPC) [2–4]. The EAD-TEPC measures the lineal energy spectra (y) in a range from 0.2 to 2000 keV/µm [2]. The TEPC spherical chamber has an inner diameter of 50 mm and is surrounded with a tissue equivalent plastic (A-150) sphere with a thickness of 3mm. The chamber is filled with tissue-equivalent gas to simulate a site size of 1 µm diameter. The TEPC raw data is measured with three gains (low, medium, high gain with 1024 channels each) and from this the lineal energy spectrum is calculated with a resolution

Please cite this article as: U. Straube, T. Berger and M. Dieckmann, The ESA Active Dosimeter (EAD) system onboard the International Space Station (ISS), Z Med Phys, https://doi.org/10.1016/j.zemedi.2023.03.001

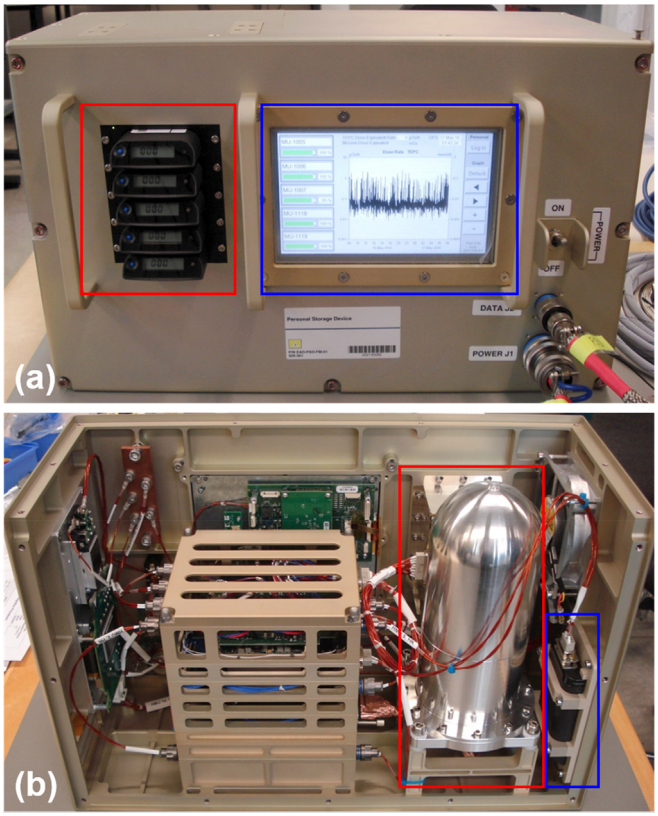

Figure 1. (a): The EAD-PSD Flight Model (FM) with five EAD-MUs inserted into the EAD-MU-reader-head (in red) and the touchscreen display (in blue), (b): The EAD-PSD, open view from the back, with the EAD-TEPC framed in red and the EAD-iMU framed in blue.

Figure 2. The five FMs of the EAD-MUs.

of 120 bins covering the lineal energy regime from 0.2 to 2000 keV/µm.

The second in-built radiation detector is the internal EAD-MU (EAD-iMU) (see back side of the EAD-PSD in Fig. 1b) and further on Section 2.1. The EAD-MU-reader-head enables the charging of the EAD-MUs internal rechargeable batteries as well as the readout of the EAD-MU housekeeping (H/K) and science data. The touchscreen display additionally allows the visualization of the current EAD-MU status (battery charging status). In addition, the

Please cite this article as: U. Straube, T. Berger and M. Dieckmann, The ESA Active Dosimeter (EAD) system onboard the International Space Station (ISS), Z Med Phys, https://doi.org/10.1016/j.zemedi.2023.03.001

touchscreen provides access to the dose rate measured with the EAD-TEPC located within the EAD-PSD.

All the EAD data from the active radiation detectors as well as all the internal H/K data of the system are stored once per day at midnight in preparation for data downlink.

2.1 EAD-MU

The following Section 2.1 discusses the operational aspects of the EAD-MUs in Section 2.1.1 and describes the relevant radiation detectors as implemented and applied within the EAD-MUs, in Section 2.1.2.

2.1.1 EAD-MU: The operational aspects

Fig. 2 shows the five FMs of the EAD-MUs as designed, built and deployed within the EAD project. The relevant operational features of the EAD-MUs are listed in Table 1. A single EAD-MU has the dimension of $93 \times 58 \times 17\ mm^3$, a mass of 120 g, is powered with an in-built rechargeable battery (1100 mAh) and equipped with a display with various functions as a push button and an LED at the front side. Four connectors at the EAD-MU back side provide interfaces for a) EAD-MU charging upon insertion into the EAD-MU-reader-head and b) for data readout.

The EAD-MU display enables three visualization modes: a) in case of assigned personalization, an indication of the astronaut dedicated three-digit identification code (Astronaut-ID), or if not as Fig. 2 displays: “000”, b) the current dose equivalent rate in μSv/h and c) the acquired cumulative dose equivalent in mSv from start of the measurement, until readout. Pressing of the blue push button at the left front side of the EAD-MU, sequences the three display mode functions. Pressing the button for more than 2 s, sets to standard display function. The right display side at the EAD-MU-front-side, houses additionally a LED, which function as battery low charge level warning at a defined limit. Two distinct warning functions prevail: a) battery warning: the system works nominal, however, requires recharge within the next 48 h, b) battery alarm, in case the battery approaches near discharge. However, then data will be stored with a subsequent nominal system shut down. The LED-blinking frequency at the MU front left side indicates mode status on either battery alarm or mere warning, urging for an immediate required charge.

Table 1
EAD-MU – Overall summary table.

Dimension	$93 \times 58 \times 17\ mm^3$
Mass	120 g
Power	1100mAh Li-ion battery
Radiation detectors	Thick silicon diode
	Thin silicon diode
	Instadose©
	RadFET
Display functions I	Astronaut ID
	Mission dose (mSv)
	Dose equivalent rate (μSv/h)
Display functions II	Battery warning
	Battery alarm
Data rate/day	140 kB
Time resolution	300 s
Operational time	10.5 days

For the ISS application, all data of the EAD-MUs are stored within a five-minute integration interval in the internal non-volatile flash memory, including the science data generated by the four radiation detectors, i.e. thin and thick diode, Instadose© and RadFET, as well as H/K data such as internal voltages and temperatures.

2.1.2 EAD-MU: The applied radiation detectors and their properties

The EAD-MU houses four different radiation sensors to determine relevant radiation protection quantities. The four sensors are a combination of two silicon diodes, a thick silicon diode (300 μm) and a thin silicon diode (7 μm), as well as an Instadose© Direct Ion Storage (DIS) ionization chamber [5–7] and a RadFET detector. The relevant characteristics and measurement variables of these detectors are listed in Table 2.

Firstly, focus will be given on the two Si-diodes, which compromise a combination of two silicon detectors further denoted as thick diode (300 μm) and thin diode (7 μm). The relevant energy deposition ranges (E_{Dep} in Si) are 0.055–16.496 MeV for the 300 μm thick diode and 0.194–27.613 MeV for the 7 μm thin diode. The energy depositions are plotted in 32 equidistant logarithmic bins for both diodes. The relevant energy depositions in these total 64 bins are the primary raw data stored by both diodes. For absorbed dose and subsequently, dose equivalent determination, the data from the two diodes is combined as following. Based on calculations of the particle average mean path length traversing detectors in 4π (352 μm for the thick and 10.4 μm for the thin diode) the energy deposition spectra are converted to the Linear Energy Transfer (LET) spectra in H_2O, attributing the thick diode as low LET, and the thin diode as high LET spectral detector. For this, and to allow for a sampling overlap between the diodes, the bins used for the thick diode reduce to 26 with an LET range from 0.09 to 10.03 keV/μm and the bins for the thin diode down to 31 with a LET range from 10.3 to 1470 keV/μm. By this means, the thick and thin diode provide the combined absorbed dose values, as well as the combined dose equivalent values, following the Q versus LET relationship as provided in [8]. In this sense the combination of the thick and the thin diode can be compared to the combination of thermoluminescence (TLD) and nuclear track etch detectors (CR-39) applied in space radiation dosimetry [1,9] where the TLD acts as the

Please cite this article as: U. Straube, T. Berger and M. Dieckmann, The ESA Active Dosimeter (EAD) system onboard the International Space Station (ISS), Z Med Phys, https://doi.org/10.1016/j.zemedi.2023.03.001

Table 2
Major physical sensor properties of the EAD-MU.

Detector	Diodes			Instadose©	RadFET
	Thick	Thin	Thick + Thin		
Thickness (μm)	300	7	-	-	-
Area (cm^2)	0.3	0.3	-	-	-
Average path length (μm)	352	10.4	-	-	-
Count rate (HITS)	X	X	X	-	-
Energy bins (log)	32	32	64	-	-
E_{Dep} (Si) (MeV)	0.055–16.496	0.194–27.613	-	-	-
LET (keV/μm) (H_2O)	0.09–10.03	10.3–1470	0.09–1470	-	-
$\dot{D}(H_2O)$	X	X	X	X	-
D (Si) (μGy) (cum)	-	-	-	-	X
$\dot{H}(H_2O)$ (μSv/h)	-	-	X	-	-

low LET detector and the CR-39 provides the high LET data. Additionally, the thin diode is equipped with a 0.9 mm polyethylene cover, to convert neutron contributions to charged particles, which cause detectable signals within the thin Si-diode [10–12]. In addition, the third EAD-MU integrated radiation sensor complements these measurements. The Instadose© device, based on the DIS detector system developed by Mirion [5–7], is a small ionization chamber providing the cumulative absorbed dose in H_2O. It was already demonstrated that the DIS-system has a LET efficiency very close to one for all LET values up to a few hundred keV/μm [13]. In this sense, the Instadose© operates also as a second absorbed dose measurement device and delivers data that compare contiguous to the absorbed dose measured with the thick and thin diode combined. At the current time Instadose© systems are for example nominally applied in hospitals as personal radiation detectors [7].

The fourth EAD-MU-detection system, the RadFET as provided by the Tyndall National Institute (Tyndall), Cork, Ireland, provides high dose response measured as absorbed dose in Si for a possible Solar Particle Event (SPE) with a lower detection threshold of a few mGy with efficiency mostly for protons. The measured data is therefore comparable to the absorbed dose in Si for the thick diode.

2.2 EAD: Calibrations

Various laboratories around the world served the calibrations of the EAD-TEPC and the EAD-MUs. Calibrations with ^{137}Cs and ^{60}Co were performed at the Seibersdorf Laboratories (SL), Seibersdorf, Austria, with neutrons at the Physikalisch Technische Bundesanstalt (PTB), Braunschweig, Germany with a) 1.2 and 14.8 MeV monoenergetic neutrons, and b) with ^{241}AmBe and ^{252}Cf sources and c) at iThemba, South Africa, for neutron energies up to 200 MeV/n. Radiation hardness testing via proton exposure, took place at the Paul Scherrer Institute (PSI), Villigen Switzerland. For the simulation of the galactic cosmic radiation environment, irradiations took place at the Heavy ion Medical Accelerator (HIMAC) facility of the National Institute of Radiological Sciences (NIRS) in Chiba, Japan. The HIMAC irradiations enabled comparison of all EAD-MU detectors, i.e. thin-, thick diodes, Instadose©, RadFET with data generated by the EAD-TEPC.

Exemplarily Fig. 3 provides data for the calibrations with heavy ions at NIRS, Chiba, Japan in Fig. 3a (EAD-MUs) and Fig. 3b (EAD-TEPC). Irradiations at HIMAC were performed with protons (230 MeV/n), Helium ions (150 MeV/n), Carbon ions (400 MeV/n), Neon ions (400 MeV/n), Silicon ions (490 MeV/n) and Iron ions (490 MeV/n). Fig. 3a shows the LET-distribution for the EAD-MUs for these ions and energies. The LET was derived, based on the nominal incidence of particles on the 300 μm thick and the 7 μm thin diode. While the thick diode data covers the protons and the helium ions, the thin diode data takes over at around 10 keV/μm and provide data for the heavier ions up to iron. In comparison Fig. 3b provides the y*d(y) spectra as measured by the EAD-TEPC for the same ions and energies.

Calibrations with monoenergetic neutrons (1.2 and 14.8 MeV) as performed at PTB, Braunschweig, Germany for the EAD-TEPC are given in Fig. 3c (1.2 MeV) and Fig. 3d (14.8 MeV). These Figures provide the relevant y*d(y) and y*h(y) spectra for the EAD-TEPC clearly showing the differences in the relevant monoenergetic neutron exposures with an average quality factor <Q> as measured for the 1.2 MeV neutrons of 16.2 and 7.7 for the 14.8 MeV neutrons.

3 EAD on-board the ISS

3.1 The Short Duration Mission (SDM): EAD-MUs

As part of the Short Duration Mission (SDM) “iriss” of ESA Astronaut, Andreas Mogensen two EAD-MUs flew to the ISS in September 2015. For this endeavor, the EAD-MUs were charged at the launch site in Baikonur

Please cite this article as: U. Straube, T. Berger and M. Dieckmann, The ESA Active Dosimeter (EAD) system onboard the International Space Station (ISS), Z Med Phys, https://doi.org/10.1016/j.zemedi.2023.03.001

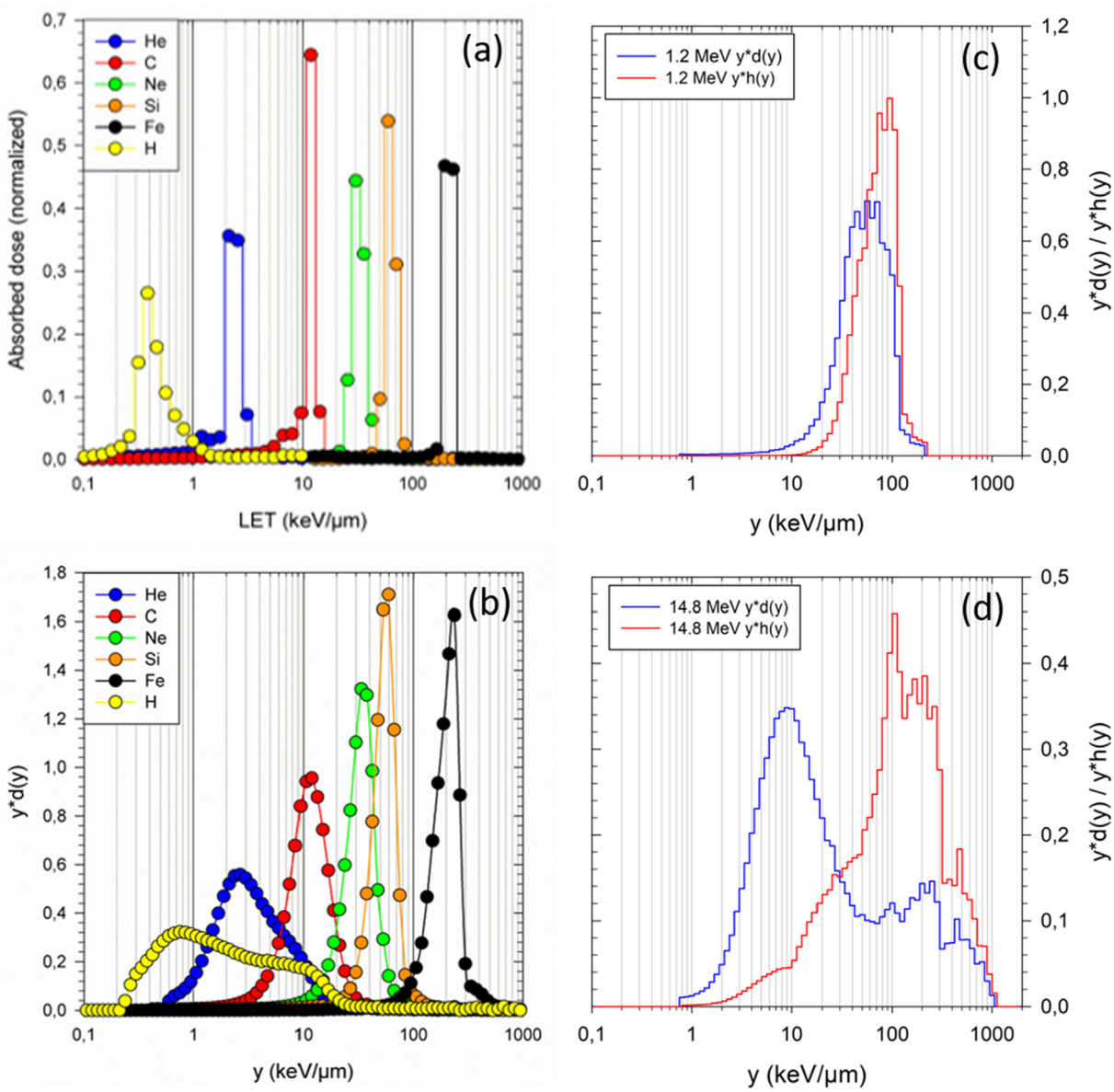

Figure 3. Exemplarily results for the EAD system calibrations. (a): thick and thin diode LET distribution after heavy ion calibrations at HIMAC, Chiba, Japan, (b): ESA-TEPC y*d(y) distributions for the same ions and energies as in (a), y*d(y) and y*h(y) distribution for monoenergetic neutrons (c): 1.2 MeV and (d): 14.8 MeV as measured at PTB, Braunschweig, Germany.

and stowed in the Soyuz spacecraft shortly before the launch on 01 September 2015. After arrival on the ISS, the units were taken to ESA's Columbus laboratory (see Fig. 4). After completion of the "iriss" mission, the two units were stowed back in the Soyuz capsule for the return to Earth a day before undocking and descent.

After landing, the dosimeters were immediately brought on board the same flight used for the direct return of Andreas Mogensen from Kazakhstan to the ESA-EAC in Cologne/Germany. The analysis of the EAD-MU data took place on September 13, 2015 at DLR, as further described in Section 4.

To the authors' knowledge, this was the first spaceflight in which an active, battery-powered radiation detector recorded the radiation environment of a complete mission in all phases: Measurements on the ground before launch, during launch and ascent aboard the Soyuz capsule, during docking as well as transfer to the ISS, throughout the duration of the mission aboard the ISS, during return to the lander and descent, return to Earth, including landing and

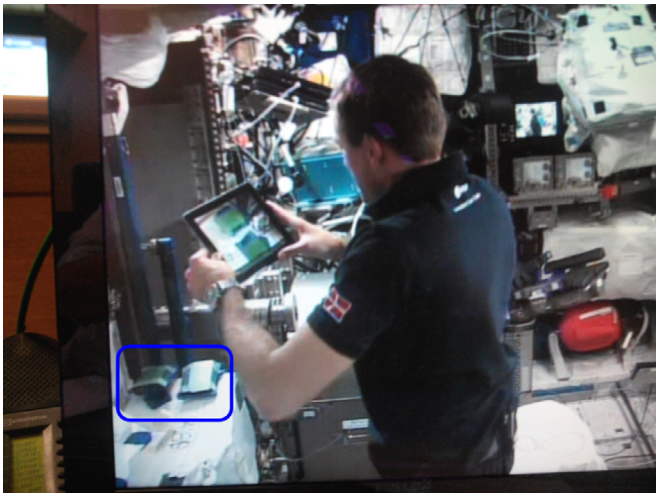

Figure 4. ESA astronaut, Andreas Mogensen, photographs the two EAD-MUs in their blue Nomex© pouches on-board the Columbus Laboratory of the ISS © ESA.

recovery from the Soyuz capsule. The ESA SDM "iriss" of Andreas Mogensen brought a total of two EAD-MUs into space and onboard the ISS. The measurements of these two EAD-MUs concluded the first part of the EAD technology demonstration (TechDemo) in space.

3.2 The full EAD system onboard the ISS

The second and final part of the ESA TechDemo began with the deployment of the complete EAD system, consisting of the EAD-PSD and five EAD-MUs. For this purpose, the EAD system was launched into space on 18 July, 2016, aboard the SpaceX-9 cargo ship. Transfer to the ISS and the installation of the EAD-PSD in the Columbus module were successfully completed by the Japanese astronaut Takuya Onishi on 28 July, 2016 (see Fig. 5). This as prerequisite for the second part of the TechDemo, which was later accomplished by the ESA astronaut Thomas Pesquet (see also Section 3.2.1).

Using ESA's 28 V Portable Power Supply (PPS), the EAD-PSD served both as a stand-alone detector unit and hub for storing, displaying, and transmitting EAD-PSD data, as well as for servicing and charging the EAD-MUs. The PPS itself was powered by a 120 V SUP outlet (SUP3/4) from Columbus, while Port 8 of the Hirschman switch served as the data interface for downloading the acquired dosimetry data and transmitting it to the ground station.

Nominal data downlink, performed once a week via ESA's Columbus Multi-Purpose Computer and Communication (MPCC) data interface, allowed a secure sftp connection to the onboard system. At midnight of each day, the corresponding science data and the data of the so-called H/K system together with the corresponding md5 checksum were compressed into a zip file and stored for downlink.

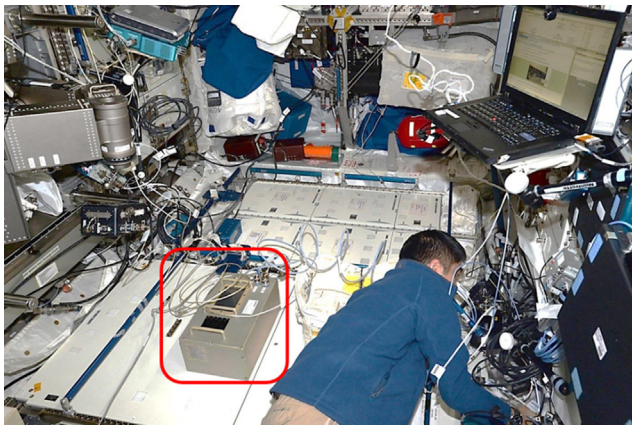

Figure 5. JAXA astronaut, Takuya Onishi, during installation of the EAD system in Columbus © ESA.

Downlinks for the commission phase of the EAD, i.e. downlink #1–#4, relayed via the Center for the Development of Activities in Microgravity and Space Operations (CADMOS) in Toulouse, France. For the operational phase of EAD, i.e. downlink #5–#47 the Centre of Crew Operations Support (CoCOS), now replaced by the EAC Crew Operation Support (ECOS) served as user center at the ESA-EAC Cologne, Germany.

The installation of the Muscle Atrophy Research and Exercise System (MARES) experiment required a relocation of the EAD-PSD during the EAD mission inside the Columbus Laboratory. Fig. 6, Table 3 and Fig. 7 depict the ISS locations of the EAD-PSD and the respective timeframes of operation.

Please cite this article as: U. Straube, T. Berger and M. Dieckmann, The ESA Active Dosimeter (EAD) system onboard the International Space Station (ISS), Z Med Phys, https://doi.org/10.1016/j.zemedi.2023.03.001

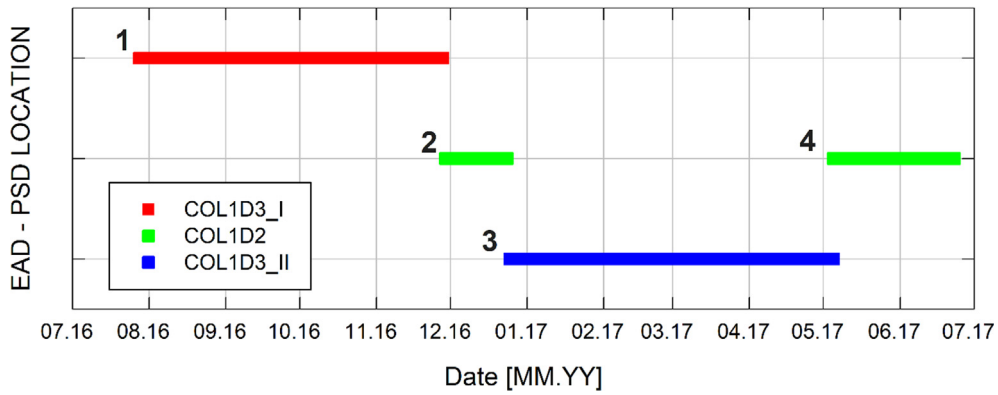

Figure 6. EAD-PSD locations inside the Columbus Laboratory during the timeframe of the EAD mission (28 July 2016 to 24 June 2017).

Table 3
EAD-PSD locations inside the Columbus Laboratory with detailed start, end Day of Year (DoY) and operational duration in days.

PSD	Location	Start [DoY]	End [DoY]	Start Date	End Date	Duration [Days]
1	COL1D3_I	209	332	28.07.2016	28.11.2016	123
2	COL1D2	332	360	28.11.2016	25.12.2016	28
3	COL1D3_II	360	125	25.12.2016	05.05.2017	131
4	COL1D2	125	172	05.05.2017	24.06.2017	50

Knowing the exact location of the EAD-PSD within the Columbus module is important because the average shielding properties in the vicinity of the EAD-PSD may change depending on its mounting place. This in turn would lead to differences in the measured radiation field parameters, as described in Section 5.

3.2.1 EAD-MUs: TechDemo Personal Dosimeters

One focus of the TechDemo of the EAD by European astronaut Thomas Pesquet during his "proxima" mission was to review all critical functional and operational aspects of the entire EAD system as they interact. For example, proper operation of the detectors and EAD-MU readout controls, measurement data storage and downlink to the ground station, charging, and touchscreen functions including data display options were verified. The basic functions of the EAD system for usage of the EAD-MUs as personalized dosimeters are further explained in the following: Each astronaut is assigned an individual, unique 4-digit code before using an EAD-MU. The astronaut must log in with his personal code via the touch screen display of the EAD-PSD. After that, all EAD-MUs inserted into the EAD-MU-reader-head at that time will be personalized for that exact astronaut. This in turn means that the astronaut could now take any EAD-MU from the EAD-PSD as his personal, i.e. specifically assigned EAD-MU. After an astronaut has taken one EAD-MU from the EAD-MU-reader-head, the system automatically logs that person out, and all EAD-MUs remaining will be anonymized immediately. This process is then repeated in the same way when the next astronaut logs in, e.g., to receive a freshly loaded personal dosimeter, to read and/or store data, to transmit and/or to display data.

In the standard utilization as a personal dosimeter, the corresponding EAD-MU is brought back to the EAD-PSD after one week of usage by the astronaut concerned. By inserting this still personalized EAD-MU into EAD-MU-reader-head, all data of this EAD-MU is automatically read out and stored for this exact astronaut. At the same time, the EAD-MU has already started to charge. After initialization and charging by the EAD-PSD, the EAD-MU is ready for use again. Prior to the mission of Thomas Pesquet, the procedures of personalization for three EAD-MUs (with Astronaut ID) was successfully tested as part of the EAD systems commissioning phase. Three units were personalized and applied as area monitors in the Columbus and the Leonardo module (see Section 3.2.2).

Thomas Pesquet (see Fig. 8) started the TechDemo activity on 21 November, 2016 lasting till his return to Earth in June 2017. A total of twenty-seven periods of individual measurements were conducted using the EAD-MUs as the crew's personal dosimeters at various locations on the ISS. The relevant EAD-MUs, with their applied color codes and personalized during the TechDemo activity, are shown in Fig. 9.

Please cite this article as: U. Straube, T. Berger and M. Dieckmann, The ESA Active Dosimeter (EAD) system onboard the International Space Station (ISS), Z Med Phys, https://doi.org/10.1016/j.zemedi.2023.03.001

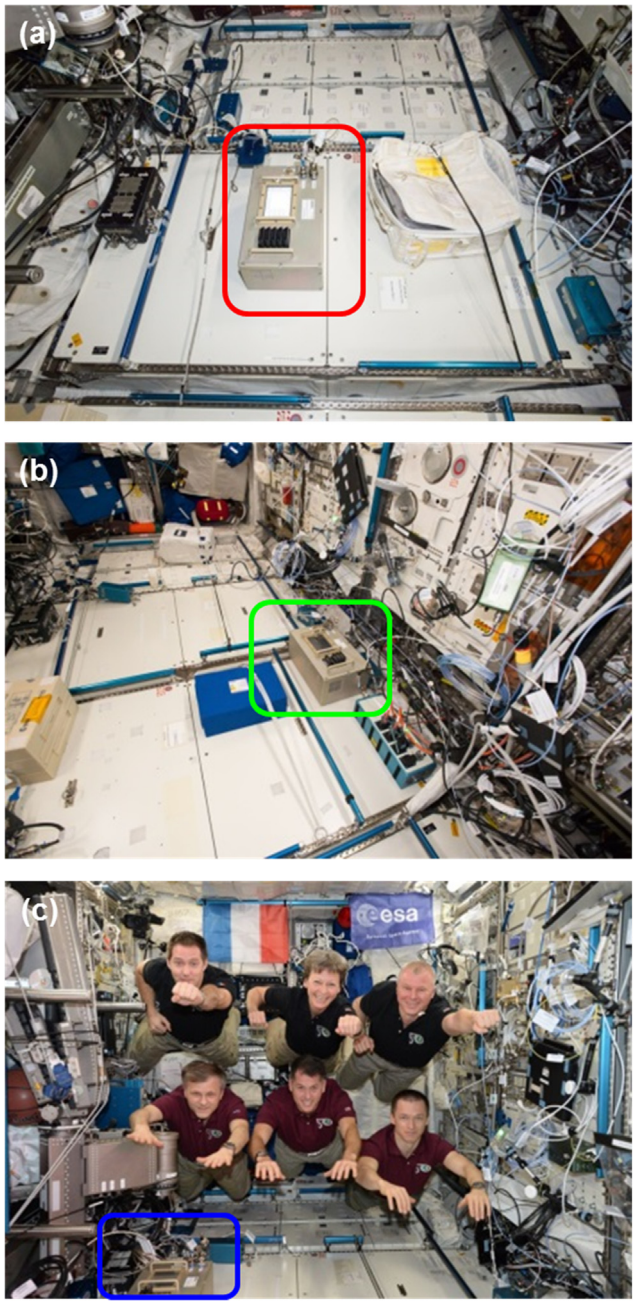

Figure 7. Locations of the EAD-PSD in the Columbus Laboratory. (a): COL1D3_I, (b): COL1D2, (c): COL1D3_II, © ESA. NOTE: Color-coded frames reflect the locations as given in Fig. 6.

3.2.2 EAD-MUs: Area Monitoring

One additional investigation conducted with the EAD-MUs on board the ISS was the usage of the EAD-MUs as area monitors and for that reason fully charged EAD-MUs were removed from the EAD-PSD, placed in Nomex© pouches and mounted at fixed locations for a planned nominal duration of about two weeks.

Thereafter the respective EAD-MUs returned into the EAD-MU-reader-head for subsequent battery charging, data readout and data downlink. Fig. 10 shows the timeline and the seven locations used for the area monitoring with the EAD-MUs. Two locations positioned in the Columbus Laboratory, two locations in the Leonardo Module, one location in the sleeping quarter in the US Orbital Segment (USOS) as well as two locations in the sleeping quarters of the Russian Segment in the Service Module (Zvezda) were chosen for this endeavor. The respective time and placement of the EAD-MUs for these seven sites are provided in Table 4.

Fig. 11 exhibits some example pictures of the EAD-MUs placed at locations in the Columbus Laboratory (Fig. 11a and d), in the US part of the ISS (Fig. 11b), in the Leonardo Module (Fig. 11e) and in the Russian Service Module (Fig. 11c and f).

During the entire EAD TechDemo in space a total of twenty-three area monitoring experiments were conducted aboard the ISS, resulting in a record of radiation data equivalent to a total of 281.7 days in LEO (see Table 4).

4 EAD-MUs: Data Short Duration Mission (SDM)

The following Section 4 discusses data measured with the two EAD-MUs during the ESA SDM "iriss" of ESA astronaut Andreas Mogensen in September 2015, starting with an overview over the whole mission, providing relevant data in Section 4.1 and then investigating the influence of the Soyuz Altimeter on the readings of the EAD-MUs upon installation in Soyuz for return the Earth in Section 4.2. As explained in Section 3.1, batteries of the two EAD-MUs (P/N 1005 and 1006) received full charging in Baikonur prior to the installation into Soyuz. The EAD-MUs, then measured until full battery discharge, and all the measured data was stored safely on the non-volatile flash memory. Table 5 provides an overview of the start and end times of the measurements for the two EAD-MUs. The EAD-MU 1005 charged at first, thereby starting the measurements 9 h 35 min earlier (at 03:27 UTC) than EAD-MU 1006 (at 13:02 UTC). Both EAD-MUs measured for almost the same amount of time: 10.85 days for EAD-MU 1005 and 10.87 days for EAD-MU 1006 leading to an operational delta time of some 0.5 hours.

4.1 EAD-MU: SDM – Science Data for the mission

Fig. 12, provides the science data overview as acquired by both EAD-MUs, showing in panel (a) and (c) the count rates (cts/min) measured with the combination of the thick and thin diode.

Further, on the absorbed dose rates (μGy/h) for the combination of the thick and thin diodes are provided in panel

Please cite this article as: U. Straube, T. Berger and M. Dieckmann, The ESA Active Dosimeter (EAD) system onboard the International Space Station (ISS), Z Med Phys, https://doi.org/10.1016/j.zemedi.2023.03.001

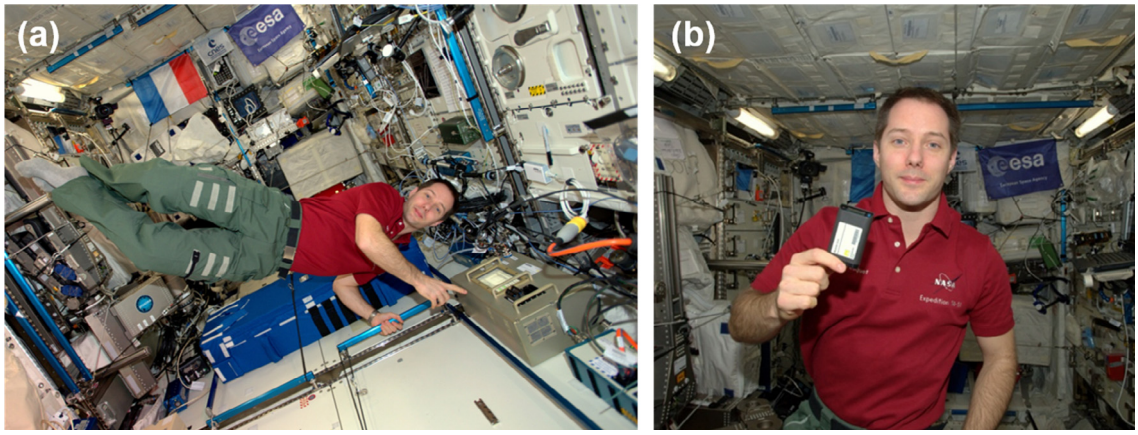

Figure 8. (a): ESA astronaut, Thomas Pesquet, with the EAD-PSD, (b): Thomas Pesquet with one of the personalized EAD-MUs applied during his TechDemo personal dosimeter study © ESA.

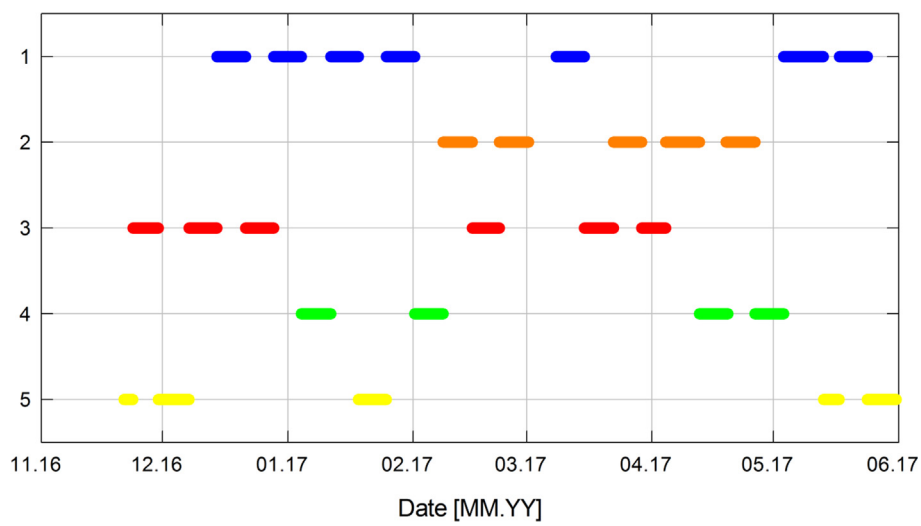

Figure 9. EAD-MUs as applied by Thomas Pesquet for his mission. The plot-ordinate-indicated-numbers, 1 to -5 refer to the internal serial number (S/N) of the used EAD-MUs.

(b) for MU 1005 and panel (d) for MU 1006. As derivable, data of both EAD-MUs are quite similar in the count- and dose rate values. The only clear difference, is that MU 1005 stopped the measurements shortly before midnight on 11 September, 2015 while MU 1006 enabled the "full circle" by providing data upon to the return to Earth on 12 September, 2015. For a differentiated view on the various mission phases, focus is now on the data generated with the thick diode of the MU 1006. The count- and dose rate profiles are given in Fig. 13a (cts/min) and Fig. 13b (µGy/h) respectively.

The applied color-code in Fig. 13 shows the measurements of MU 1006 during the nine different phases of the SDM. Those are described in Table 6 that gives information on the respective location of the dosimeters as well information on date, time and duration of the measurement for each phase of the "iriss" mission.

The results of the dosimetric measurements during different phases of the mission and the corresponding locations of the detectors (as given in Table 6) are further detailed: Phase 1 as the natural radiation background at Baikonur Cosmodrome, Kazakhstan. Phase 2 stowage onboard the Soyuz Capsule on top of the Soyuz rocket which still resides on ground. Phase 3 as the actual space flight began with launch and ascent. Phase 4 Soyuz capsule had been docked to ISS. Phase 5 at the Columbus module, i.e., after transit of the dosimeters form Soyuz to the ISS. Phase 5 marks the longest period of continuous exposure measurements in space at a single location onboard ISS, in the frame of the "iriss" mission and the first phase of ESAs TechDemo. This measure-

Please cite this article as: U. Straube, T. Berger and M. Dieckmann, The ESA Active Dosimeter (EAD) system onboard the International Space Station (ISS), Z Med Phys, https://doi.org/10.1016/j.zemedi.2023.03.001

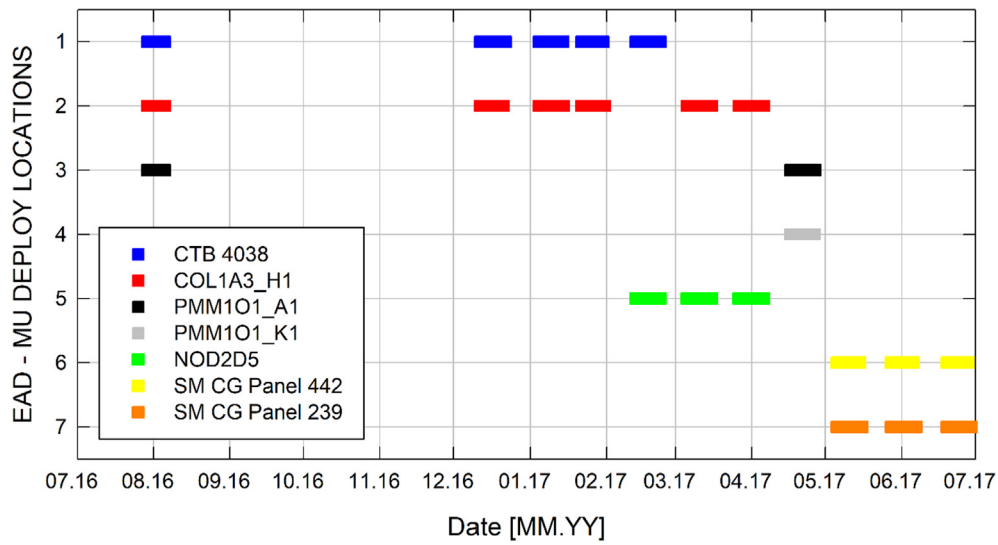

Figure 10. Operation time and locations for the placement of the EAD-MUs as area monitors onboard the ISS.

Table 4
Locations of the EAD-MUs at the selected sites within the ISS with the respective number of measurement runs and the total measurement period in days.

#	Module	Location	Number of runs	Duration [Days]
1	Columbus	CTB 4038	5	46.68
2		COL1A3_H1	6	56.87
3	Leonardo	PMM1O1_A1	2	17.41
4		PMM1O1_K1	1	9.81
5	NODE2	NOD2A1	3	30.29
6	Zvezda	SM CQ Panel 442	3	30.34
7		SM CQ Panel 239	3	27.27

ment cycle could collect data of ∼6.2 days in total, while the dosimeters were located in the Columbus module. On the last day of this period, the EAD-MUs were returned to be stored on Soyuz for their return to Earth. This defined Phase 6. In contrast, Phase 7 comprised of the measurements that took place during descent of Soyuz and rapid return to Earth. Dosimetric data of Phase 8 though were collected on Earth again and essentially correspond to the dose from the natural background radiation at the landing site in Kazakhstan. Beyond that, data of exposure could even be collected during the crew's helicopter flight on return of crew and hardware from the landing site to the recovery station. That defined phase 9.

The following Fig. 14 quantifies further the nine different mission phases for MU 1006 and the respective six mission phases for MU 1005 by providing data for the thick diodes. Fig. 14 shows in panel (a) and panel (c) the count rate versus dose rate for the MU 1005 and the MU 1006. Panel (b) and (d) provide the energy deposition spectra for the two EAD-MUs. The differentiation between the various mission phases (as given in Table 6) is clearly visible and supports the statement, that depending on the relevant radiation environment the data can be clearly separated.

4.2 EAD-MU: SDM – The Altimeter

An interesting detail of the resolved field data property is the sudden increase in count- and dose rate upon the EAD-MU installation in Soyuz for deorbit, prior to departure from the ISS, as already shown in Fig. 13 (in black) and in Fig. 14 (in black). For a better comparison, attention is exclusively on count rates and absorbed dose rates, measured by the thick diode of the MU 1005. Fig. 15 provides for the MU 1005 the count rates (Fig. 15a), the dose rates (Fig. 15b) as well as the counts/energy bin/day (Fig. 15c) and the dose/energy bin/day (Fig. 15d) for Columbus and Soyuz respectively. The pedestal onset at installation in Soyuz is clearly visible and it also shows in Fig. 15c and d as an increase in the lower energy depositions in Si up to ∼400 keV.

It stands to reason that the raise detected by the EAD-MUs is due to the γ-ray altimeter hard mounted within the

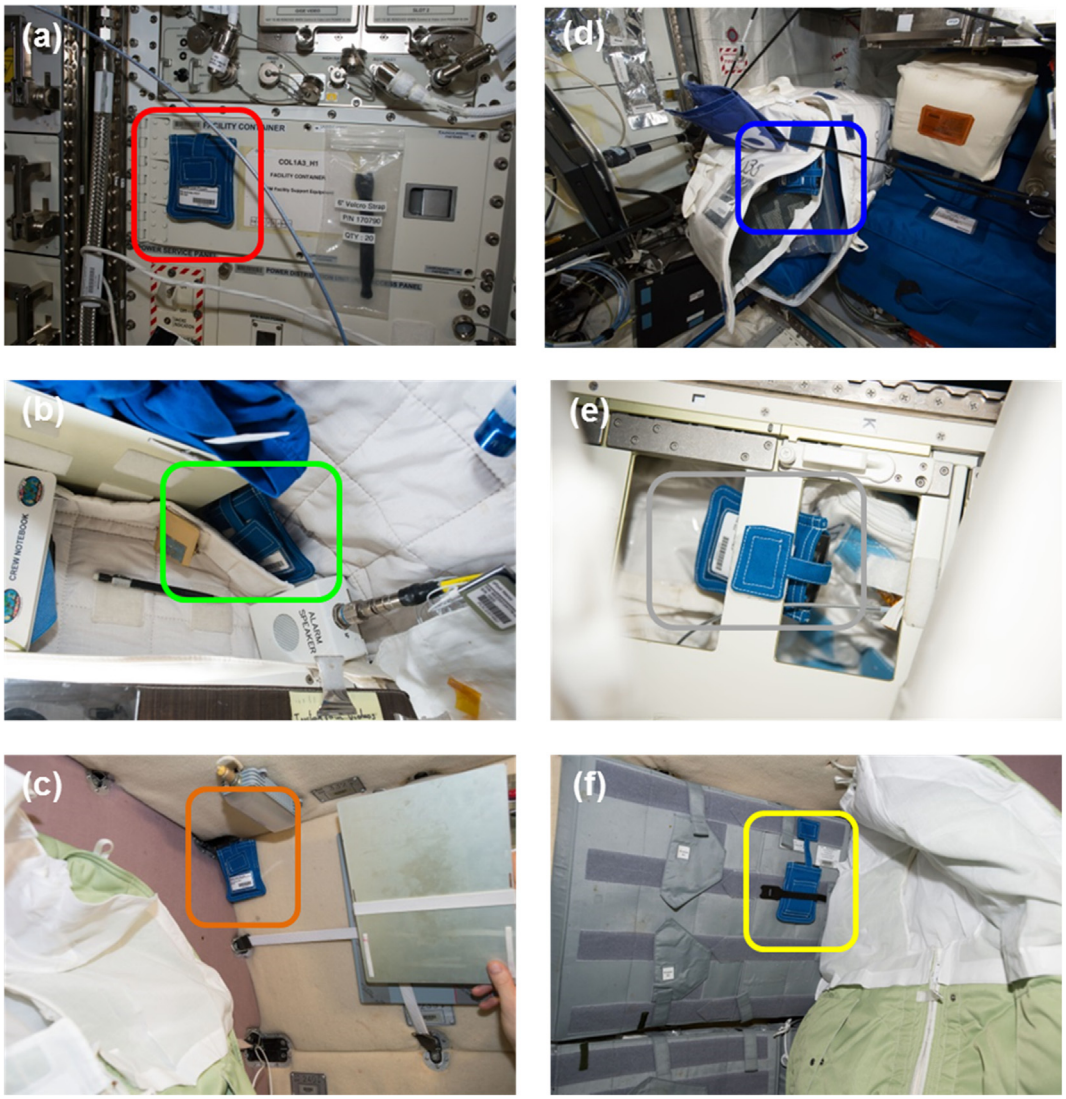

Figure 11. The EAD-MUs at some of their selected area monitoring locations. NOTE: Indicated color-coding bases on locations provided in Fig. 10 © ESA.

Table 5
Performed measurement periods for the EAD-MU 1005 and EAD-MU 1006.

MU	Serial Number [S/N]	Start Time	End Time	Duration	
		[UTC]		[Days]	[Hours]
1005	001	01.09.2015 03:27	11.09.2015 23:52	10.85	260.42
1006	002	01.09.2015 13:02	12.09.2015 09:57	10.87	260.92

Soyuz capsule which is used to cushion the impact on the ground during landing to protect the crew and equipment. Table 7 shows dose and dose rate measured during a particular day (09 September, 2015) by the EAD-MUs on Columbus and Soyuz (11 September, 2015. Furthermore, an estimated average is lined out, assumed to be attributed to the γ-ray altimeter. Prerequisite to be taken for granted is that any other circumstance able to interfere with the envi-

Please cite this article as: U. Straube, T. Berger and M. Dieckmann, The ESA Active Dosimeter (EAD) system onboard the International Space Station (ISS), Z Med Phys, https://doi.org/10.1016/j.zemedi.2023.03.001

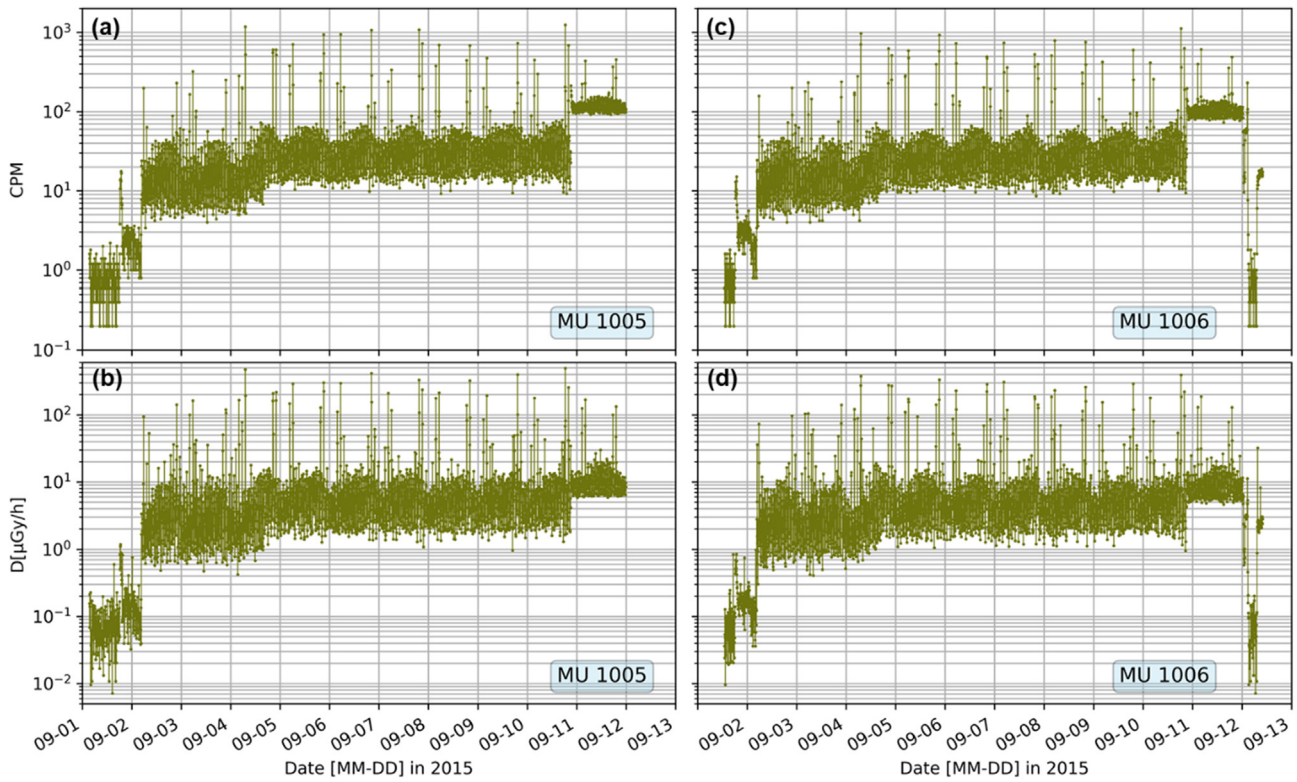

Figure 12. Count rate (cts/min) and absorbed dose rate (μGy/h) for the MU 1005 in (a) and (b) and for the MU 1006 in (c) and (d).

ronmental exposure significantly, can be excluded. An additional dose of roughly ∼ 96 μGy/day would have attributed to the γ-ray source within Soyuz.

5 EAD: Data ISS Mission

Section 5 contains sample data from measurements of the complete EAD system onboard the ISS, during the period from July 2016 to June 2017. This period essentially corresponds to ESA's space mission "proxima" (launch 17 November 2016, landing 02 June, 2017) of ESA astronaut Thomas Pesquet and marks the second, final phase for ESA's TechDemo. However, the actual precise starting point of phase two of the ESA's EAD TechDemo began with the dawning and activation of the EAD system by JAXA astronaut Takuya Onishi in July 2016. Section 5.1 will provide a brief overview of the data generated by the EAD-TEPC. Section 5.2 presents the data gathered by the EAD-iMU over a period of one-year. Section 5.2 includes data comparison from all detector systems embedded within the EAD-MUs, namely the thick and thin diode, the Instadose© and the RadFET detector. Section 5.3 shows a comparison of the data measured by the EAD-MUs that were used as area monitors. For this purpose, data from the Columbus laboratory as well as from the Leonardo module of the ISS are presented. At the end of Section 5, we compare in Section 5.4 the EAD-iMU data with data from a different experiment onboard ISS called DOSIS 3D.

5.1 EAD: ISS – EAD-TEPC

Section 5.1 reviews the data generated with the EAD-TEPC for a one-month period from 21 May to 21 June 2017. At this period the EAD-PSD was located at position COL1D2 (see also Fig. 7b) close to the European Physiology Module (EPM) rack in Columbus. The EAD-TEPC's lineal energy spectra and the respective count rate data are stored with a one-minute time. From this raw data, the absorbed dose values and the dose equivalent values are calculated. Fig. 16 provides an overview of two days of EAD-TEPC data generated in June 2017. Fig. 16 provides in (a) the count rates, in (b) the absorbed dose rates and in (c) the dose equivalent rates. For better comparisons of the absorbed dose rates and the respective dose equivalent rates the ordinate scale in Fig. 16b and Fig. 16c culminates with a maximum of 2000 μGy/h and 2000 μSv/h, respectively.

For better data quantifications, the EAD-TEPC data for a one-month time period under study is further provided in Fig. 17, in dependence on the L-values [14], the vertical geomagnetic cut-off rigidity (R_C) and the latitude of the ISS. For the calculation of the R_C, the approximation of Smart and

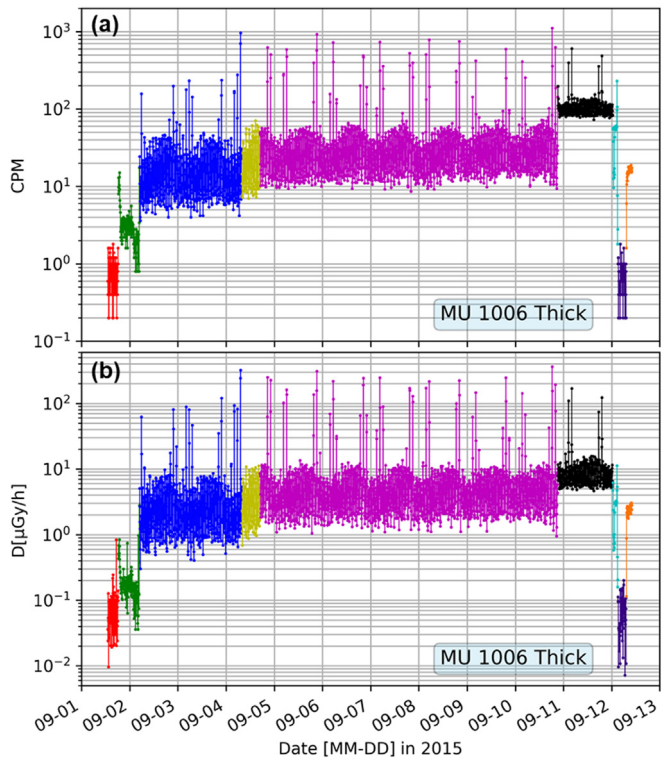

Figure 13. (a) Count rate (cts/min), (b): absorbed dose rate (μGy/h) for the MU 1006 for the full mission duration. NOTE: Data visualizes the data from the thick silicon diode within the EAD-MU.

Table 6
The nine SDM phases in September 2015 and measurement durations for the MU 1006.

Phase	Location	Start	End	Duration [days] MU 1006
1	Baikonur	01.09. 13:02	01.09. 17:58	0.206
2	Installed in Soyuz	01.09. 18:03	02.09. 04:39	0.442
3	Soyuz to the ISS	02.09. 04:40	04.09. 07:41	2.126
4	Soyuz docked to ISS	04.09. 07:46	04.09. 16:42	0.372
5	Inside Columbus	04.09. 16:47	10.09. 21:04	6.179
6	Soyuz docked to ISS	10.09. 21:09	12.09. 00:51	1.114
7	Return to Earth	12.09. 00:56	12.09. 02:56	0.083
8	Kazakhstan	12.09. 03:01	12.09. 07:07	0.171
9	Helicopter flight	12.09. 07:12	12.09. 09:57	0.206

Shea [15] with $R_C = 14.5/L^2$ was applied (see also [16]). Fig. 17 provides in (a), (b) and (c) the absorbed dose values in dependence on L, R_C and latitude and in (d), (e) and (f) the relevant dose equivalent data for the three before mentioned parameters. The contributions from the crossings of the SAA, regarding L values below two, are clearly visible within absorbed dose values ranging up to 1000 μGy/h during SAA maxima. The GCR attributed maximum values of absorbed GCR dose of up to 20 μGy/h equal at L values around six. Similar conditions can be observed for the data in dependence on R_C and on the latitude of the ISS with an SAA maximum at roughly −28° south. Comparison of the absorbed dose and the dose equivalent values reveal, the latter having a higher spread in the data with maximum values of up to 2000 μSv/h for SAA crossings and up to 100 μSv/h for the maximum GCR dose values. This is plausible as the quality factor calculation commence for each minute of data.

In addition to the correlation of the count-, dose- and dose equivalent rates with the L, the R_C and the latitude data, one may of course also correlate the measured data with the orbit of the ISS. The relevant orbit correlation of the EAD-TEPC

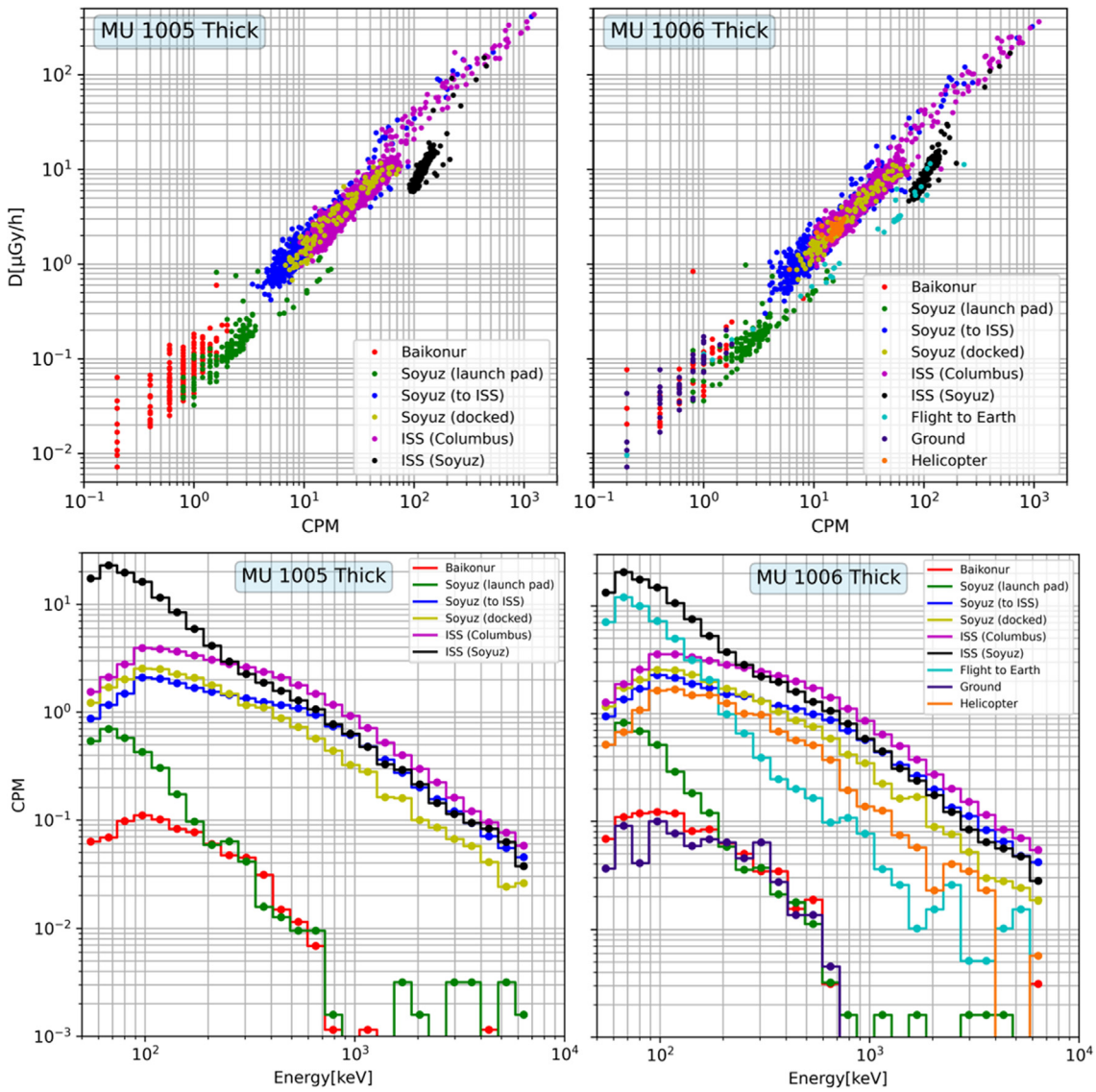

Figure 14. Count rate (cts/min) versus dose rate (µGy/h) for: (a) MU 1005 and (c) MU 1006 for the full SDM; energy deposition spectra for: (b) MU 1005 and (d) MU 1006 also for the full SDM. NOTE: Data shown refer to the data from the respective thick silicon diodes of both EAD-MUs.

data for the one-month time period under study is given in Fig. 18, providing in (a), (b) and (c) the orbit correlated count rate, absorbed dose rate and dose equivalent rate with the same ordinate scale as given in Fig. 16. With this representation, the focus is on the SAA and the respective SAA crossings.

Fig. 19 provides the same data, as in Fig. 18b and c, however, with a limitation on the ordinate scale for the absorbed dose in (a) of 100 µGy/h, as well as for the dose equivalent in (b) of 100 µSv/h, showing clearer the relevant GCR variations over the orbit of the ISS. In addition, panel (c) provides the calculated average quality factor ($Q_{AVERAGE}$) (for data summarized in 10° latitude and 6°longitude intervals) for the relevant orbit segments. Fig. 19c gives an indication of the variation of $Q_{AVERAGE}$ with the orbit segment showing especially the clear depression of $Q_{AVERAGE}$ while the ISS passes through the SAA which attributes to the dominance of protons with lower average LET in the SAA (see further Fig. 21).

Based on the correlations and observations so far, the following passage provides the relevant absorbed dose and dose equivalent values for the one-month time period under

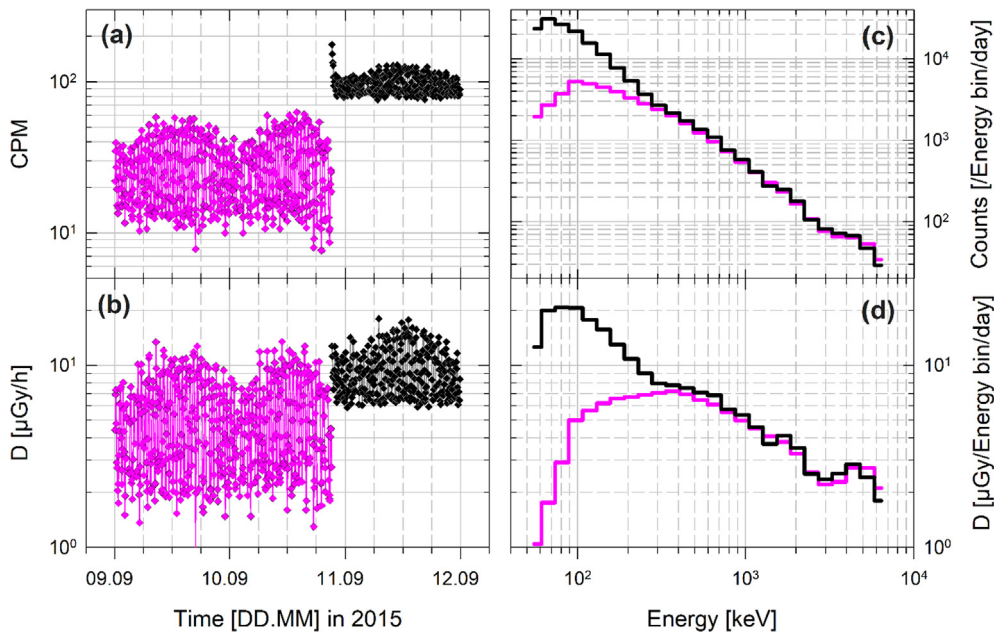

Figure 15. (a): count rates (cts/min), (b): dose rate (µGy/h), (c): counts per energy bin/day, (d): absorbed dose per energy bin/day for the MU 1005 for Columbus (purple) and for Soyuz (black). NOTE: only thick diode and only GCR data.

Table 7
The GCR dose data in Columbus on 09 September 2015 and in Soyuz on 11 September 2015 together with the respective dose contribution from the Soyuz Altimeter.

MU	S/N	Columbus	Soyuz	Altimeter		Altimeter (average)	
		[µGy/day]		[µGy]	[µGy/h]	[µGy]	[µGy/h]
1005	001	117.2	219.1	101.9	4.25	96	4
1006	002	107.4	197.6	90.2	3.76		

study. To achieve this the orbit correlated absorbed dose and dose equivalent values have been separated in the GCR and SAA contributions. The relevant daily absorbed dose values as well as dose equivalent values are therefore provided in Fig. 20 showing in (a) the total daily absorbed dose and dose equivalent values and in (b) and (c) the respective contributions for GCR and SAA.

The data synopsis to Fig. 20 elaborates further in Table 8, showing the average daily dose rates and the dose equivalent rates for SAA, GCR and the sum of both. The daily-absorbed dose values for SAA (168 ± 14 µGy/day) and GCR (146 ± 2 µGy/day) are close to each other. The dose equivalent values for SAA (300 ± 25 µSv/day) and GCR (457 ± 9 µSv/day) differ by more than 50% due to the difference of the mean quality factor for the SAA (1.78 ± 0.03) dominated by trapped protons and secondary neutrons) and for GCR (3.14 ± 0.04).

In summary, a daily-absorbed dose of 314 ± 14 µGy/day and a daily dose equivalent of 758 ± 24 µSv/day with an average Q of 2.41 ± 0.04 was measured for example in the June-2017 period.

To further compare the relevant GCR and SAA contributions as measured with the EAD-TEPC additional data is provided in Fig. 21. Fig. 21 shows the daily measured absorbed dose and dose equivalent values versus the lineal energy (y) for GCR (Fig. 21a) and SAA contributions (Fig. 21b). The daily dose values are based on the average daily values as given in Table 8. The comparison clearly shows the higher dose equivalent contributions for the GCR in comparison to the SAA as well as the higher low lineal energy contributions for the SAA crossings.

To finalize the EAD-TEPC data evaluation, the intention is to investigate the quality factors, as shown in relation to the ISS orbit in Fig. 19c. Here, the absorbed dose and dose equivalent data in dependence on R_C (as shown in Fig. 17b and e) was at first separated for the GCR and SAA contributions and then re-binned to R_C intervals of 0.5 GV. The

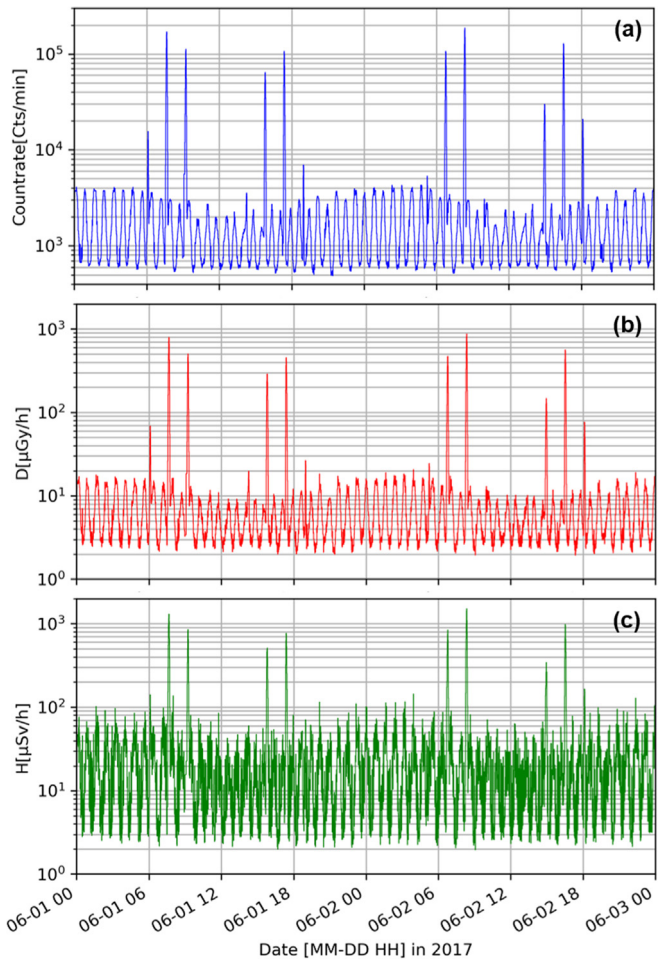

Figure 16. EAD-TEPC data for two days (a): count rate (cts/min), (b): absorbed dose rate (µGy/h), (c): dose equivalent rate (µSv/h).

results for the R_C dependence of GCR and SAA provide Fig. 22a for GCR, and Fig. 22b for SAA.

For the GCR contributions, one obtains values of up to 48.3 µSv/h for low R_C values with absorbed dose values of 14.9 µGy/h, while at the highest R_C these values decline to 7.2 µSv/h and 2.6 µGy/h, respectively. The calculation of the average Q would result in an average Q in the lowest R_C bins (from 0.5 to 2.5 GV) of $Q = 3.31 \pm 0.06$, while Q decreases to 2.76 ± 0.08 at R_C intervals from 13 to 15.5 GV. For the SAA, the peak of the SAA at 8.5 GV relates to a $Q = 1.69 \pm 0.02$, while at the "start" and the "end" of the SAA, Q values are up to 2.8 due to still small remaining amounts of GCR at these R_C values.

5.2 EAD: ISS – EAD-iMU in Columbus

After the discussion about the EAD-TEPC-data, focus is now given on the data generated with the EAD-iMU mounted inside the EAD-PSD. The EAD-iMU stores the raw data with a time resolution of 300 s every five minutes. This includes the H/K and science data from all the four detector systems: thick and thin diode, Instadose© and RadFET. Consequently, emphasis is now on the thick and think diode configuration of the EAD-iMU, followed by a comparison of the thick and think diode data with the data measured with the Instadose© and a comparison of the thick diode data with the data generated with the RadFET, which aims to be the high dose dosimeter for the EAD-system.

5.2.1 EAD: ISS – EAD-iMU Diodes

Firstly, as done for the EAD-TEPC data comparison is performed for the count rate, the absorbed dose rate and the dose equivalent rate measured, with the EAD-iMU for a respective time period onboard the ISS.

Fig. 23 provides two days of data where (a) shows the count rates in counts/min, (b) the absorbed dose rates in µGy/h and (c) the dose equivalent rates in µSv/h. As for the EAD-TEPC data, the ordinate scales for D and H are limited to 2000 µGy/h and 2000 µSv/h, respectively.

Please cite this article as: U. Straube, T. Berger and M. Dieckmann, The ESA Active Dosimeter (EAD) system onboard the International Space Station (ISS), Z Med Phys, https://doi.org/10.1016/j.zemedi.2023.03.001

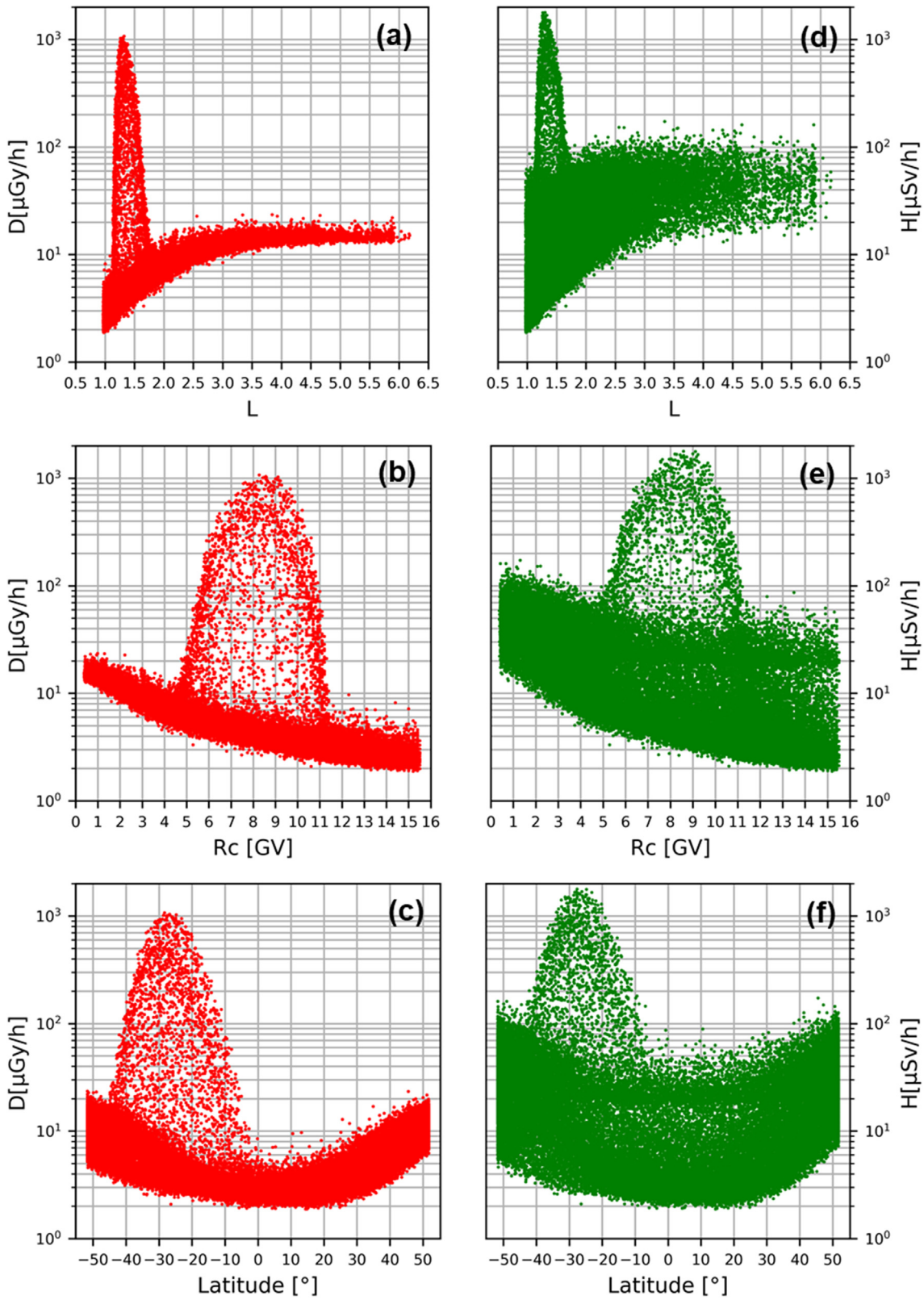

Figure 17. EAD-TEPC derived absorbed dose – and dose equivalent rates versus L (a) and (d), versus R_C in GV (Giga Volt) (b) and (e) and versus latitude (c) and (f).

Please cite this article as: U. Straube, T. Berger and M. Dieckmann, The ESA Active Dosimeter (EAD) system onboard the International Space Station (ISS), Z Med Phys, https://doi.org/10.1016/j.zemedi.2023.03.001

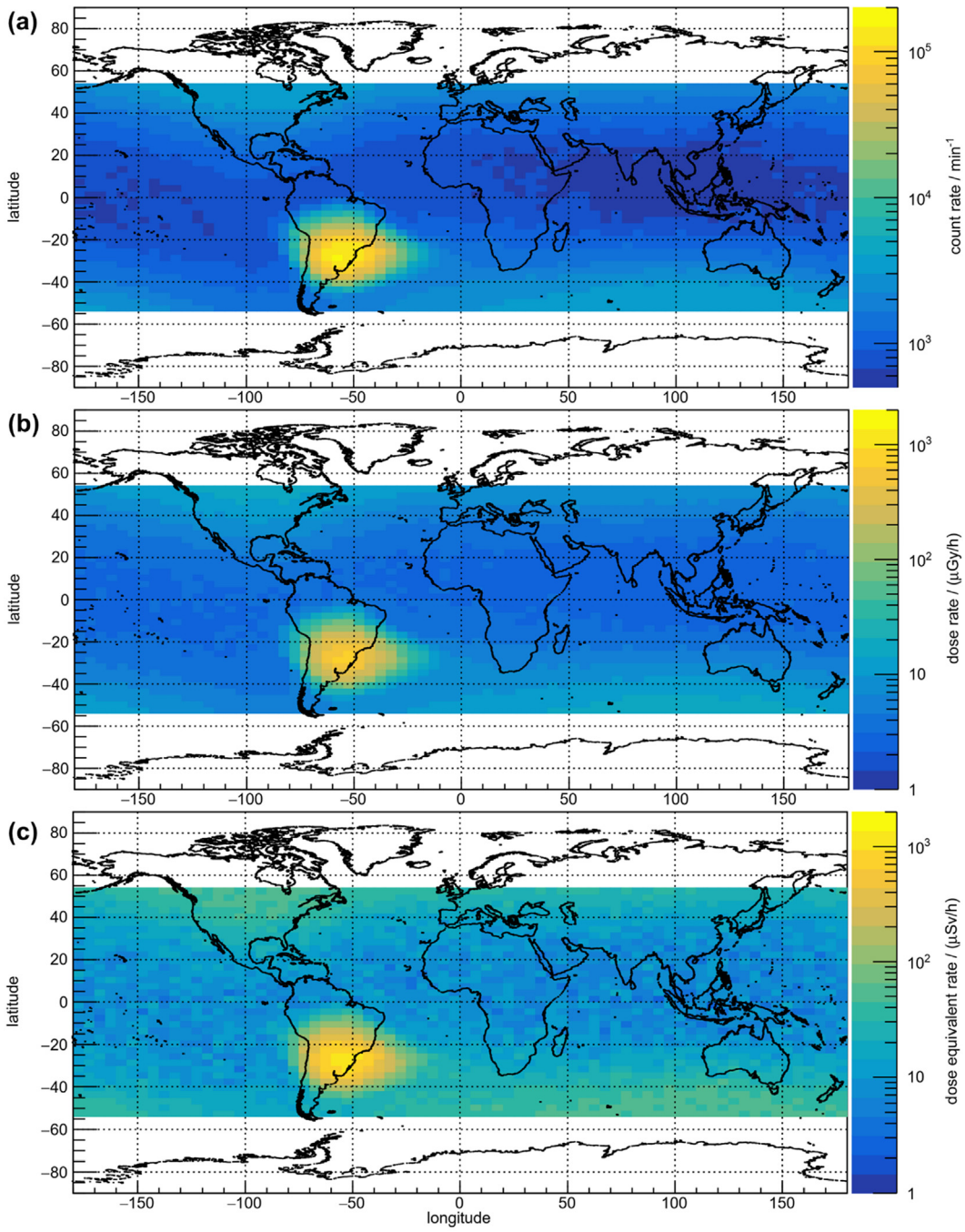

Figure 18. EAD-TEPC data for one month: (a): count rate versus orbit; (b): absorbed dose rate versus orbit; (c): dose equivalent rate versus orbit.

Next in focus is the daily data generated with the thick and thin diode configuration. As mentioned before (c.f. Table 2), the two diodes work together with the thick diode being the low energy deposition instrument (low LET detector) and the thin diode being the high energy deposition instrument (high LET detector). Fig. 24 delivers the consequences as expressed in the relevant dose values. For the data presentation in Fig. 24 the following approach is taken: at first, the dose entries for the thick and thin diode were separated either for GCR exposure or for SAA passes. Then, the relevant daily dose values for GCR and SAA were derived for the two diodes separately and for the total absorbed dose values, as given nominally, for the EAD-iMU.

Please cite this article as: U. Straube, T. Berger and M. Dieckmann, The ESA Active Dosimeter (EAD) system onboard the International Space Station (ISS), Z Med Phys, https://doi.org/10.1016/j.zemedi.2023.03.001

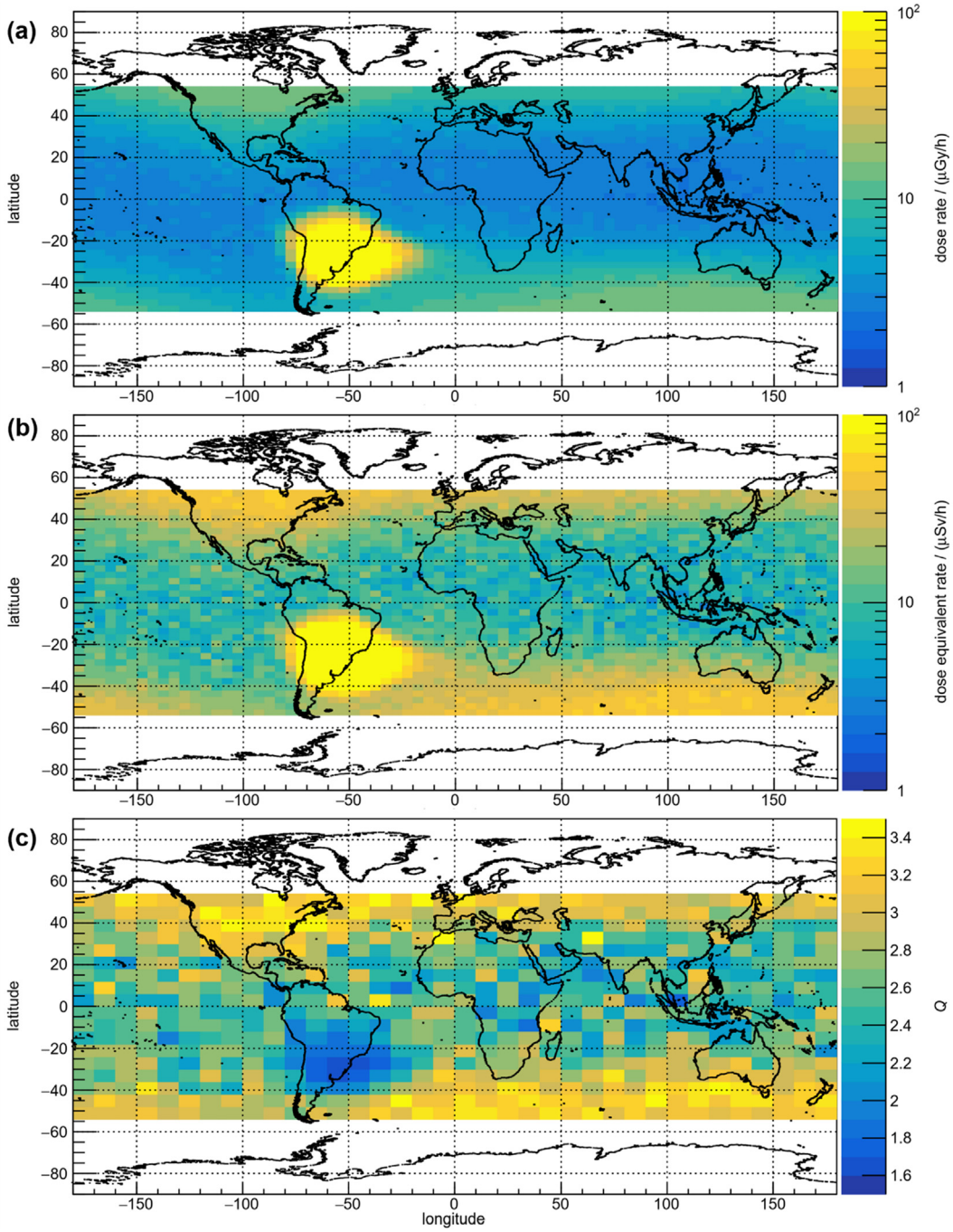

Figure 19. (a): absorbed dose rate versus orbit; (b): dose equivalent rate versus orbit; (c): quality factor measured with the EAD-TEPC over the orbit. NOTE: The practiced reduction on the ordinate of scale for the dose and dose equivalent rate, in comparison to Fig. 18 enable better comparisons of the GCR variations.

Fig. 24 thus provides the daily dose values for the GCR, the SAA and the sum of both (total): for (a) the combination of the thick and thin diode, for (b) the thick diode and for (c) the thin diode. Looking at the total daily dose values averaged over the mission, these account to 285 µGy/d for the thick and thin diode configuration, where 247 µGy/day are measured within the thick diode and 38 µGy/day for the thin diode. This implies that around 13% of the total dose is registered as high LET particles in the thin diode during the mission. Looking at Fig. 24a, and the total dose labeled in

Please cite this article as: U. Straube, T. Berger and M. Dieckmann, The ESA Active Dosimeter (EAD) system onboard the International Space Station (ISS), Z Med Phys, https://doi.org/10.1016/j.zemedi.2023.03.001

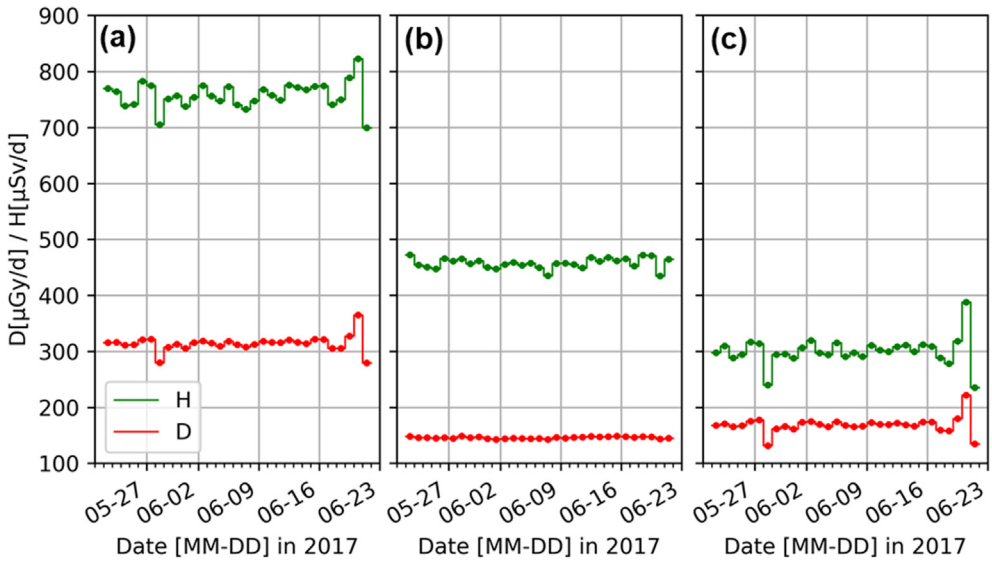

Figure 20. Daily dose equivalent in (H = green) and absorbed dose (D = red) for the total in (a); (b) for GCR; (c) for SAA.

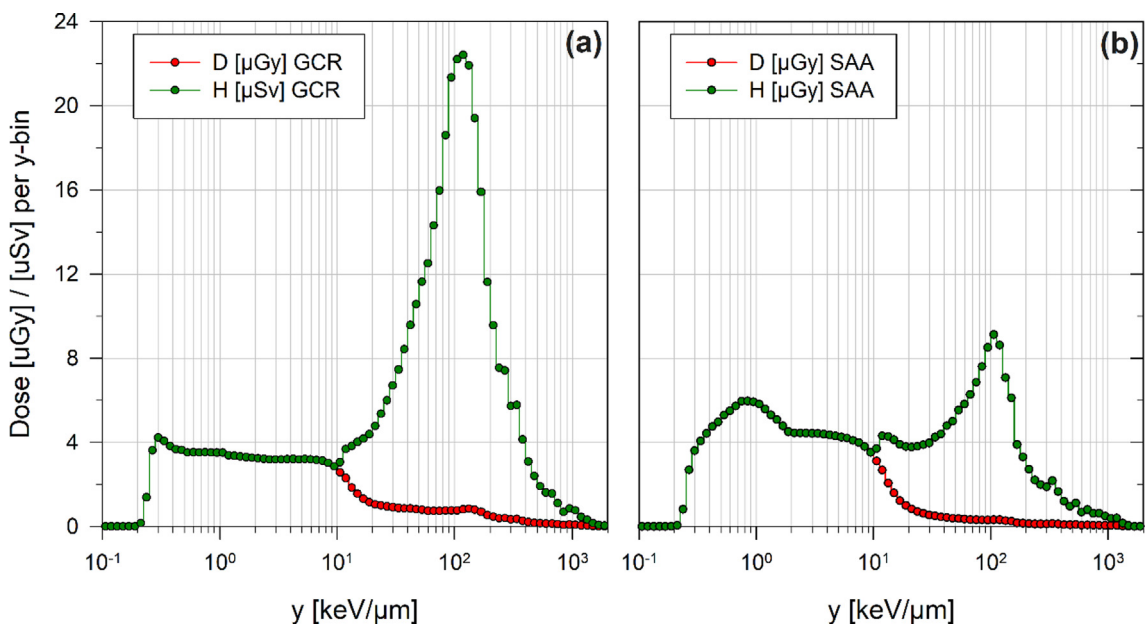

Figure 21. Daily dose equivalent in (H = green) and absorbed dose (D = red) contributions versus lineal energy (y) for (a): GCR and (b): SAA.

green (as well as the GCR dose labeled in red and the SAA dose labeled in blue), one may observe that the dose values follow to some extent a pattern. While the total dose rate is quite stable up to December 2016, it increased in December 2016, decreased again from January 2017 onwards and showed a step increase from beginning of May 2017 up to the end of the mission. The GCR-contributions (red in Fig. 24a) only very marginally increased due to decreasing solar activity, but we see a higher variation in the SAA-

Table 8
The average daily-absorbed dose (D) and dose equivalent (H) values as well as the average quality factor (Q) for the SAA and the GCR contributions together with the totals. Average uncertainty for the TEPC data at around 2%.

	D [µGy/day]	H [µSv/day]	$Q_{AVERAGE}$
SAA	168 ± 14	300 ± 25	1.78 ± 0.03
GCR	146 ± 2	457 ± 9	3.14 ± 0.04
Total	314 ± 14	758 ± 24	2.41 ± 0.04

Please cite this article as: U. Straube, T. Berger and M. Dieckmann, The ESA Active Dosimeter (EAD) system onboard the International Space Station (ISS), Z Med Phys, https://doi.org/10.1016/j.zemedi.2023.03.001

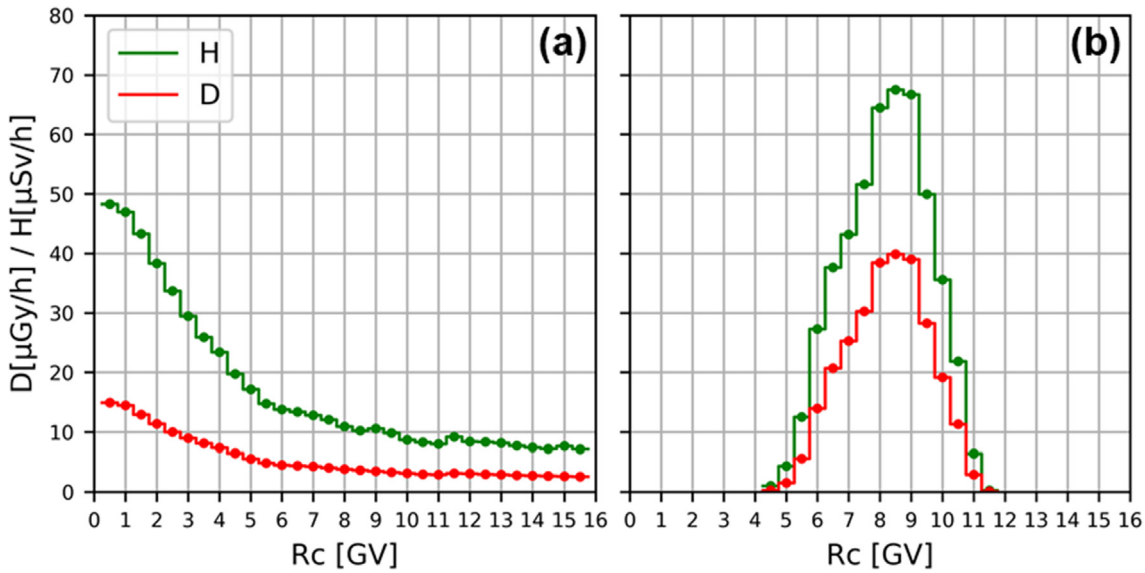

Figure 22. Dose equivalent (H) and absorbed dose (D) for (a) GCR and (b) SAA.

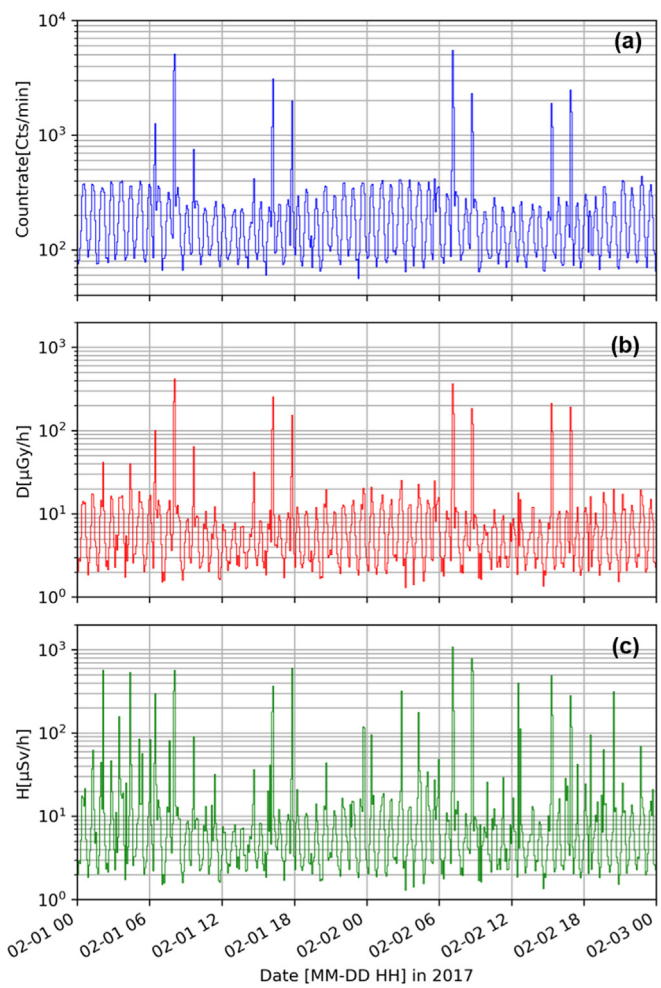

Figure 23. EAD-iMU data for two days: (a) count rate (cts/min); (b): absorbed dose rate (µGy/h); (c): dose equivalent rate (µSv/h).

Please cite this article as: U. Straube, T. Berger and M. Dieckmann, The ESA Active Dosimeter (EAD) system onboard the International Space Station (ISS), Z Med Phys, https://doi.org/10.1016/j.zemedi.2023.03.001

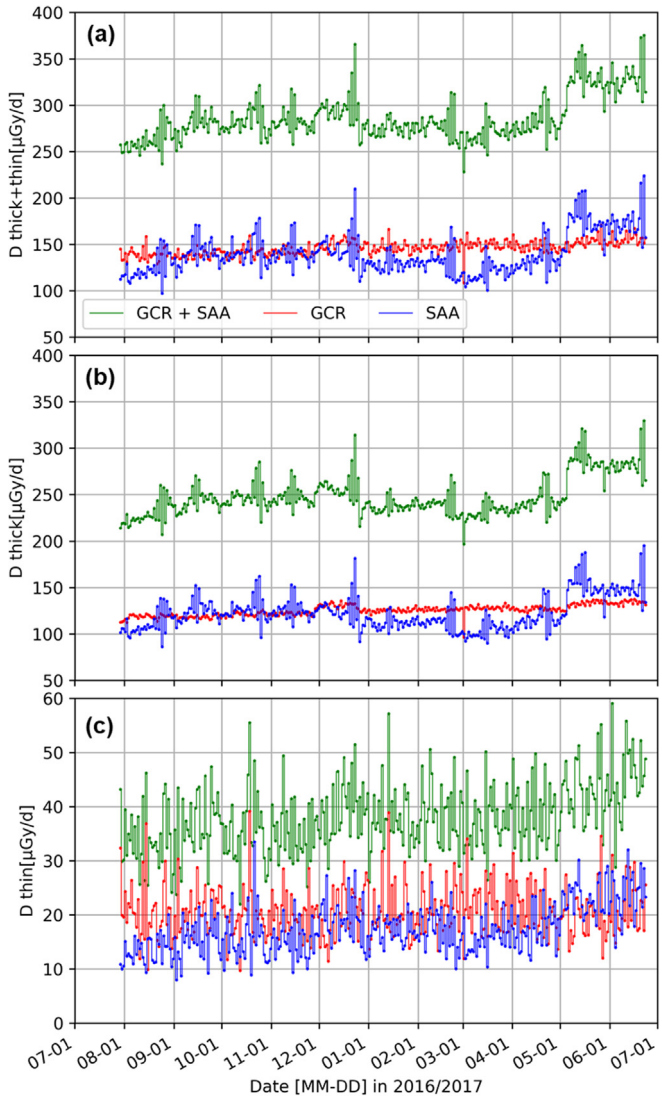

Figure 24. (a): EAD-iMU data thick and thin diode, (b): thick diode, (c): thin diode. NOTE: GCR + SAA (=total) in green, GCR in red and SAA in blue.

contributions (blue in ‘Fig. 24a). Comparing the measured SAA data with the position of the EAD-PSD in Columbus, as given in Fig. 6 and Fig. 7, acquired changes in the measured dose values are due to the position changes of the EAD-PSD inside Columbus, thereby changing the local shielding which influences the SAA contributions to a higher extend than the GCR contribution. In addition, an influence of the ISS altitude can be excluded due to the fact, that ISS altitude remained quite stable during the EAD activity at around 404 ± 1 km.

Strict data separation from entries acquired by thin and thick diode deliver the energy deposition spectra for the thick and the thin diodes for the full mission as in Fig. 25a for the thick diode separated for the SAA, the GCR and the sum and in Fig. 25b for the thin diode. While the thick diode nicely shows the GCR-spectra with the peak at around 0.1 MeV in the 300 µm diode, it also shows the shifted spectra for the SAA contributions, which culminate at around 0.3 MeV. In contrast, the thin diode energy deposition spectra follow the straight line, as expected for the high-energy depositions in the 7 µm thin diode.

5.2.2 EAD: ISS – EAD-iMU Diodes and Instadose©

The thick and thin diode configuration facilitates determination of the total dose values. The Instadose© system [5–7] within the EAD-iMU, is capable of doing this with an efficiency of approximately one for all relevant LET values (c.f. Section 2.1.2 and [13]). Therefrom, a long-term comparison of these two detector systems enables crucially two things: i) to proof that they are equivalent in measured

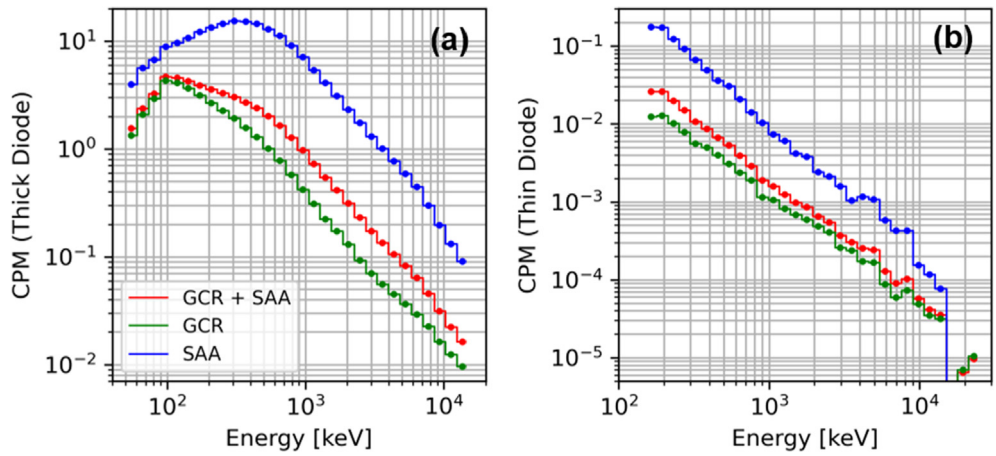

Figure 25. Energy deposition spectra for SAA, GCR and the sum for (a) the thick diode and (b) the thin diode of the EAD-iMU.

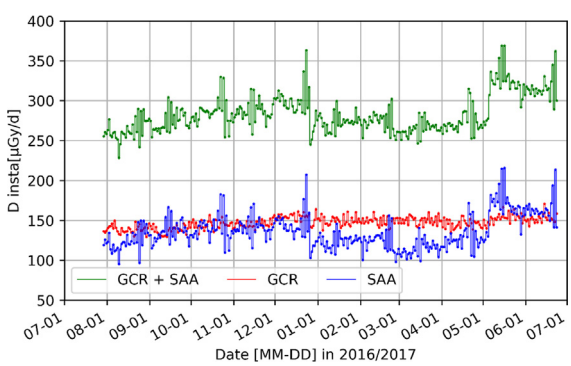

Figure 26. Instadose© daily dose values for total, GCR and SAA for comparison with Fig. 24a.

variable acquisition, and ii) to show for the first time, a long-term comparison of these two systems in space. For comparison, the data for the Instadose© has also been separated for GCR and SAA-contributions as done for the EAD-iMU. The long-term dose values, which require comparison with the data from the EAD-iMU, (as in Fig. 24a) are provided in Fig. 26. It is evident from the data, that the Instadose© detector provides a very good system in comparison, when operated simultaneously with the thick and thin diode, as in the flown complete EAD system configuration.

To enhance the data comparisons quality on the thick and thin diodes and Instadose©, data over the full mission is shown in Table 9. It gives the full mission dose and the daily dose values for the combination of the thick and thin diodes and the Instadose©. The baseline data measured from 29 July, 2016 to 23 June, 2017 spread over 328 days of data. The EAD system results match in good agreement (uncertainty ~3%) with an average dose rate for the thick and thin diode configuration of 286 ± 24 µGy/d and 283 ± 23 µGy/d for Instadose©.

5.2.3 EAD: ISS – EAD-iMU Diodes and RadFET

The RadFET detectors are part of the EAD-MUs with the intention to have one detector system, as embodied within the EAD-MU, for high dose indications as e.g. for a SPE. Nominally, the RadFET have a lower detection threshold of a few mGy in Si. Consequently, for comparison purposes, the total dose measured for all RadFETs for the respective EAD-MUs was integrated over monthly periods. Fig. 27 provides in (a) the monthly averaged data from all six RadFET-detectors within the EAD-MUs and in (b) the cumulative averaged RadFET dose compared to the cumulative thick diode EAD-iMU dose.

Table 9
Comparison of thick and thin diode and Instadose© absorbed dose in H_2O.

	Detector			
	Thick + thin diode	Instadose©	Thick + thin diode	Instadose©
	Dose (mGy)		Dose rate (µGy/d)	
SAA	43.70	42.60	133 ± 21	129 ± 21
GCR	50.10	50.40	153 ± 8	154 ± 8
TOTAL	93.80	92.80	286 ± 24	283 ± 23

Please cite this article as: U. Straube, T. Berger and M. Dieckmann, The ESA Active Dosimeter (EAD) system onboard the International Space Station (ISS), Z Med Phys, https://doi.org/10.1016/j.zemedi.2023.03.001

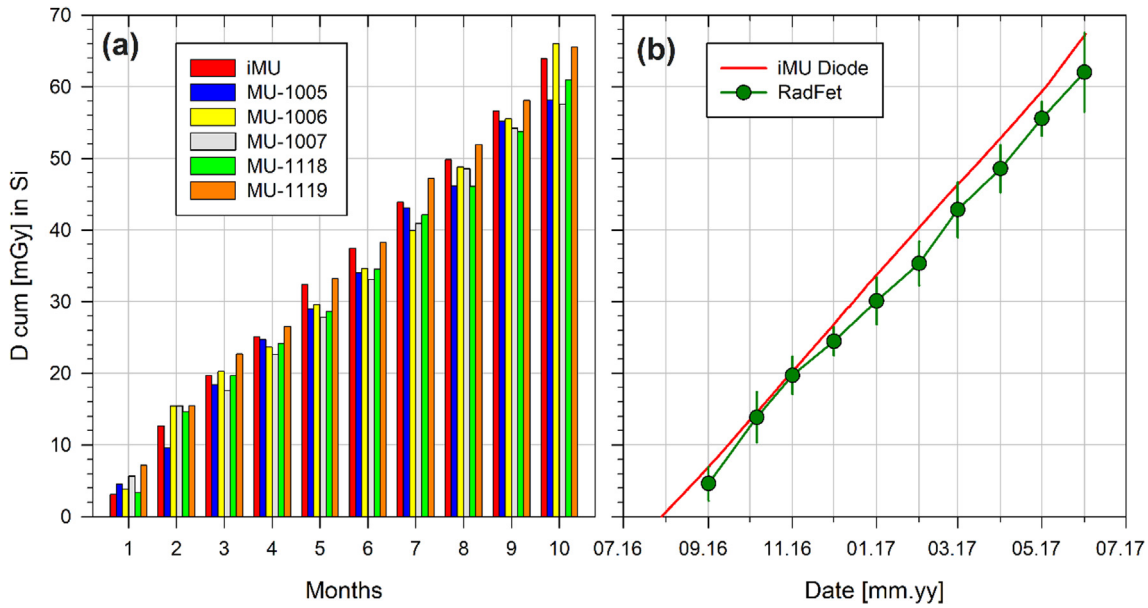

Figure 27. (a): cumulative absorbed dose in Si measured with the six RadFET detectors with an integration time of one months. (b) averaged cumulative dose for the RadFET, in green, compared to the cumulative absorbed dose in Si, measured with the thick diode of the EAD-iMU in red.

For comparison, one has to mention twofold: a) the RadFET delivers the absorbed dose in Si and b) the RadFET is mostly sensitive to protons. Ergo, RadFET data as cumulatively and averaged over six RadFETs, are compared with the cumulative dose measured with the thick diode of the EAD-iMU. Of course, one has to consider, that the thick diode not only measures protons, therefore the diode data is rather given as a guidance for the eye. Nevertheless, the cumulative does values agree within the error bars of the RadFET confirming that RadFET's respond as high dose detector for dose values exceeding tens of mGy likely to occur during a SPE.

5.3 EAD: ISS – EAD-MUs area monitoring

This section elaborates on the use of the EAD-MUs from the EAD system as area monitoring dosimeters, this also in analogy to what is stated in Section 3.2.2. As part of the TechDemo the EAD system and its EAD-MUs was also operated to determine the exposure of the environment insight ISS and its modules, which allowed e.g. to reveal subtle differences existing in shielding characteristics of the ISS. To capture such difference a high sensitivity capabilities and options for dynamic use of the dosimeters (in different location for a limited time) are relevant and those cannot be provided in such detail by passive dosimeters due to their lack of time resolution. The following provides the comparison of area monitoring data collected by the EAD-iMU in Columbus (COL1D3_II) with data of two EAD-MUs that were located in the Leonardo module at the defined positions PMM1O1_A1 and PMM1O1_K1 (see Fig. 10).

The two EAD-MUs started operation after transfer to Leonardo in April 2017. First the count rates that were measured within the Columbus module (see Fig. 28a) are compared to those obtained in the Leonardo module (see Fig. 28b) during the period of April 17–19, 2017.

Two features become obvious while assessing these graphs. First, that the count rate for SAA crossings is lower in Columbus as compared to Leonardo. Second, that the count rate minima at the geomagnetic equator are found to be elevated in the Columbus module when compared to Leonardo. Both observations relate to the specific shielding properties in these specific locations of the ISS. An increased shielding reduces the contribution of protons e.g., within the SAA. However, at the same time, the contribution of secondary radiation resulting due to the interaction of incident GCR with the stations' building material and hardware, leads to higher count rates. The interaction of different types of high energetic radiation with the shielding material manifests in variations of exposure found on ISS and so for Columbus- and the Leonardo module alluding to difference of shielding properties for the location concerned. Identical exposure characteristics are easily distinguishable, when plotting the count rate versus dose rate, which provides Fig. 29, showing the increase in SAA counts for Leonardo and the increase in GCR counts (actually a shift) for the Columbus data. A summary of daily dose

Please cite this article as: U. Straube, T. Berger and M. Dieckmann, The ESA Active Dosimeter (EAD) system onboard the International Space Station (ISS), Z Med Phys, https://doi.org/10.1016/j.zemedi.2023.03.001

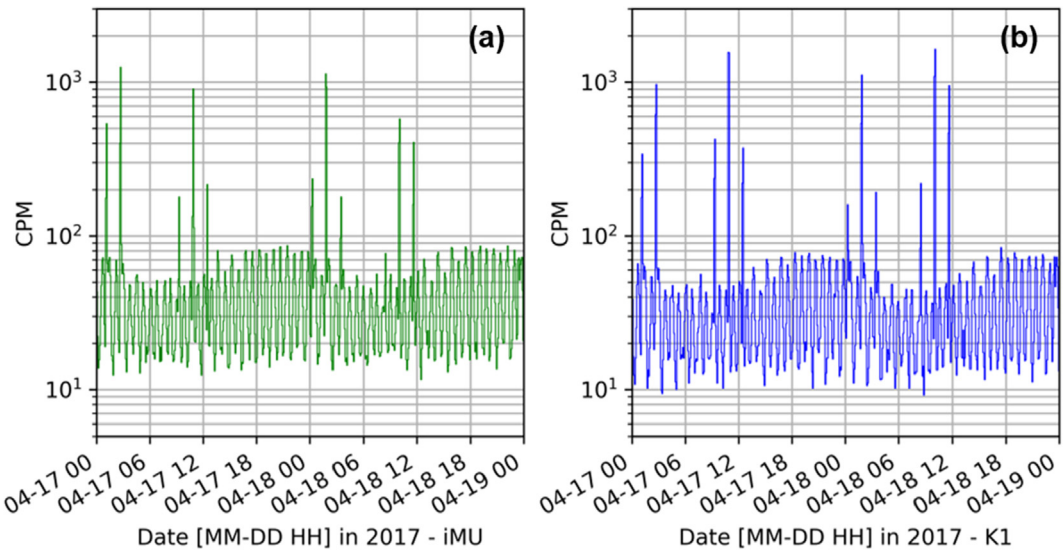

Figure 28. (a): count rate versus time for a two-day time period for the EAD-iMU in Columbus, (b): count rate profile for the EAD-MU in Leonardo at position PMM1O1_K1.

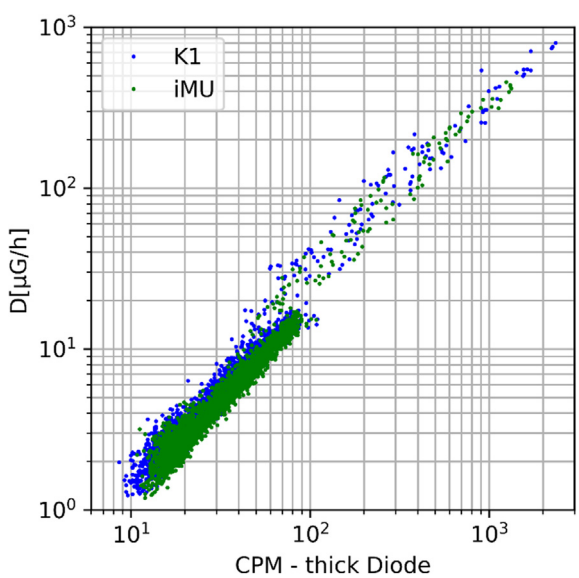

Figure 29. Count rate versus dose rate for Columbus (green) and for Leonardo (blue).

values generated for the Columbus Laboratory and the two positions in Leonardo is provided in Table 10.

For this nine-day lasting experiment, an average of 290 ± 22 µGy/day was measured in Columbus and an average of 353 ± 41 µGy/day was provided at position K1 and 369 ± 35 µGy/day at position A1 in Leonardo. The corresponding dose equivalent values were 620 ± 86 µSv/day in Columbus and 773 ± 116 µSv/day in Leonardo K1, and 799 ± 168µSv/day in Leonardo A1 respectively.

Table 10
Daily absorbed dose values in µGy/day within Columbus and Leonardo.

Date [dd. mm] in 2017	Location		
	Columbus (COL1D3_II)	Leonardo (PMM1O1_A1)	Leonardo (PMM1O1_K1)
17.04	282	394	358
18.04	299	404	364
19.04	282	379	353
20.04	314	305	281
21.04	319	378	432
22.04	252	317	333
23.04	306	395	375
24.04	271	356	325
25.04	286	380	351

5.4 EAD: ISS – EAD-iMU comparison with DOSIS 3D-DOSTEL

As indicated in Fig. 6 and Fig. 7, the EAD-PSD was relocated on 05 May 2017 to the COL1D2 location in Columbus. This location is very close to the DOSIS 3D-DOSTEL instruments [16–19], which are positioned beneath the EPM rack in Columbus. Actually, this position corresponded to the ISS-Radiation Assessment Detector (ISS-RAD) instrument in late 2017, which enabled a comparison of DOSIS 3D-DOSTEL and ISS-RAD data during the SPE in September 2017 [18]. For the purpose of this comparison, the timeframe from 01 April until 23 June 2017 served the evaluations. In April 2017, the EAD-PSD was still located at the other side of Columbus at COL1D3_II and was situ-

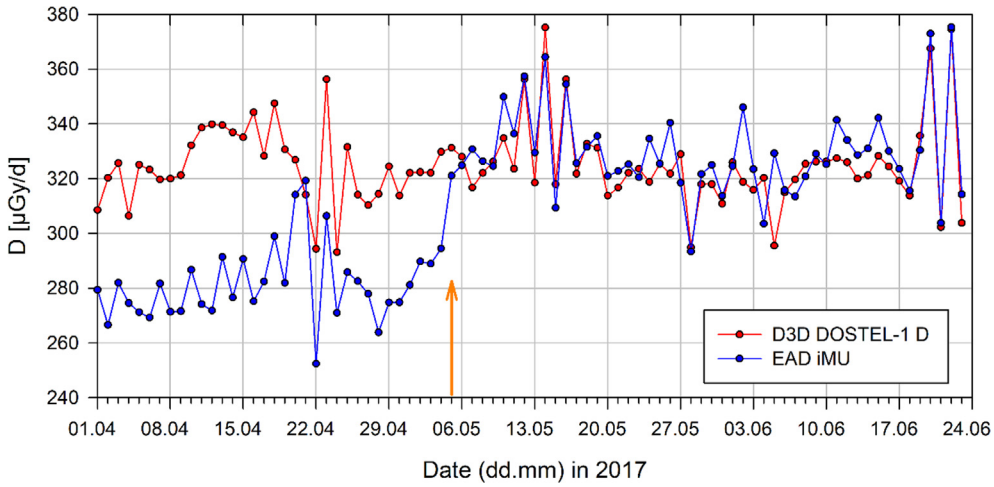

Figure 30. Comparison of the EAD-iMU absorbed dose values with the DOSIS 3D-DOSTEL-1 absorbed dose values from 01 April 2017 to 23 June 2017.

ated close to the DOSIS 3D-DOSTEL instruments on 05 May 2017. It remained at this position until the end of June 2017 offering an excellent exposure comparison location.

Fig. 30 provides the relevant data. It shows, in blue the daily-absorbed dose values measured with the EAD-iMU of the EAD system, and in red, the dose values as measured with the DOSTEL-1-instrument of the DOSIS 3D experiment. The orange arrow indicates the time the EAD-PSD was re-located close to the DOSIS 3D-DOSTEL instruments in May 2017. To provide a data baseline, the average absorbed dose rate measured with the EAD-iMU in the timeframe from 01 April to 04 May 2017 was 282 ± 14 µGy/day, while the DOSTEL-1 instrument measured 324 ± 14 µGy/-day. From the time of the re-location onwards until the 23 June 2017 the EAD-iMU acquired in average 329 ± 16 µGy/day and the DOSTEL-1-instrument 325 ± 16 µGy/day, which is in very good agreement between these two detector systems. Statistically, regarding encountered standard deviations, there is no difference. Also notable in Fig. 30 are fluctuations in the daily dose values around 13 May 2017, and around the end of June 2017. These relate to a slow shift of the SAA orbits of the ISS, having at certain time intervals a higher number of orbits during one day, when compared to the other data (c.f. the detailed description in Section 4.1.2 in [17]).

6 Conclusion

This publication describes ESA's TechDemo for testing and operating an advanced dosimetry system (EAD) capable of actively determining the exposure of the crew and environment on board a spacecraft and/or the space station to ionizing radiation.

First data were collected during the ESA's SDM "iriss" with the ESA astronaut Andreas Mogensen of September 2015 (TechDemo Phase 1). The second period of July 2016 to June 2017 further measurements on board the ISS were executed. The second period entailed the ESA mission "proxima" with the ESA astronaut Thomas Pesquet (TechDemo Phase 2).

For the "iriss" mission special attention was on the comparison of the data from two mobile dosimeters, EAD-MUs. These measurements allowed (to the author knowledge for the first time) to analyze and describe an entire space mission with dosimetric measurements for all phases of space flight. Data obtained cover on ground operations at the launch site in Baikonur, onboard the Soyuz space craft, the launch phase with ascent and flight to the ISS as well as the entire period onboard the ISS and within the European Columbus Laboratory of the ISS. Finally, measurements obtained during the return to Earth newly onboard the Soyuz capsule, the descent to landing and touch down in Kazakhstan is covered. During the TechDemo Phase 2 focus is on the EAD systems operation and performance at the ISS's Columbus Laboratory and the according data are discussed. Also, the data of the EAD-TEPC enabled for a complete comparative description including quality factor variations over all mission phases, to the authors knowledge for the first time. The advanced system of EAD-MUs encompassing four different detectors, proofed to operate accurately and reliably. Data were found to be conclusive and complemented each other. No contradictions within the data and among the different detectors systems were found. As example comparison of data from the thick and thin diodes with data obtained from the Instadose© and the RadFET detectors is provided. EAD-MUs proofed full usability beyond

Please cite this article as: U. Straube, T. Berger and M. Dieckmann, The ESA Active Dosimeter (EAD) system onboard the International Space Station (ISS), Z Med Phys, https://doi.org/10.1016/j.zemedi.2023.03.001

their prime scope of tasks namely to provide crew personal dosimetry for the individual. In regard to the conclusiveness of data among the different types of hardware for dosimetry used onboard ISS, a comparison of the EAD system with other systems on ISS and in particular with the active DOSTEL instruments of the DOSIS 3D experiment has been successfully executed and confirms and adds to the subject matter expertise.

EAD-MUs enabled for a lean operation also to assess the environmental exposures while e.g., being placed for monitoring of an area within the space station as standalone dosimeter during consecutive periods of 10 days. This mobile mapping of specific areas provided further insight into the shielding characteristics of the ISS with minimal effort. With this the EAD system also provides the benefit of increased flexibility in situations where immediate mobile surveillance is desired or demanded, e.g., substituting during periods of reduced/lost options with other standard hardware, elsewise.

In summary this paper reports on the successful execution of an ESA Technology Demonstration for entire human missions into space. ESA Medical Operations (HRE-OM) and the International Partners found the need and benefits of the dosimetry system that allows advanced active crew personal dosimetry with the additional option for mobile environmental monitoring. This adding to the capability also to cover upcoming scenarios of human spaceflight and explorations with more flexibility and augmenting radiation safety capabilities. Further testing of the EAD technology beyond low earth orbit will now be executed on the NASA Artemis 1 mission as an essential contribution of ESA to the radiation protection effort within the exploratory programs of the agencies. The next generation of the EAD system that shall entail further miniaturization, advanced interfacing and communication, lower power consumption and enhancement of ergonomics is underway.

Data Availability Statement

The code used to extract the data is distributed by the authors as open-source. The patient data can be made available on request due to privacy/ethical restrictions.

Declaration of Competing Interest

The authors declare the following financial interests/personal relationships which may be considered as potential competing interests: The paper submitted for publication exclusively deals with the Technology Demonstration (TechDemo) of the European Space Agency (ESA) Active Dosimeter (EAD) Systems for the usage in space as onboard the International Space Station (ISS).

The technology demonstrated and referred to has been patented: WO2015024591A1, US9468406, EP3036564B1 by ESA.

The following persons, Matthias Dieckmann, Ulrich Straube and Thomas Berger are the inventors. Mr. Dieckmann and Mr. Straube work for the European Space Agency (ESA), Mr. Berger for the German Aerospace Center, DLR (Deutsches Zentrum für Luft- und Raumfahrt).

To the authors knowledge no financial benefits were and/or are to be expected.

Acknowledgements

The EAD-system is product of the development phase of the European Crew Personal Active Dosimeter (EuCPAD) project, later re-named in ESA Active Dosimeter (EAD) for operational reasons, financed by ESA's optional General Supporting Technology Program (GSTP) with the continuous support by Udo Becker's as head of the GSTP program enabling one project as performed by institutions from four different European ESA member states. The EuCPAD development was carried out under ESA CONTRACT NO. 4200023059/09/NL/CP, with the project team from Austria, Germany, Finland and Ireland, namely for the Austrian Institute of Technology (AIT), Austria: Peter Beck, Marcin Latocha, Sofia Rollet, Michael Wind with support from Paolo Colautti, Davide Moro and colleagues from Instituto Nazionale di Fisica – Laboratori Nazionale di Legnaro (NFN-LNL) and for Deutsches Zentrum für Luft- und Raumfahrt (DLR), Germany: Joachim Aeckerlein, Karel Marsalek, Aleksandra Rutczynska, Daniel Matthiä, Thomas Urlings, Bartos Przybyla, Günther Reitz, for Physikalisch Technische Bundesanstalt (PTB), Germany: Marlies Luszik-Bhadra, for MIRION/ASRO, Finland: Matti Vuotila, Johanna Mäkelä, Eero Koivula, Jussi Lehti and for TYNDALL, Ireland: Alexander Jaksic.

The calibrations and irradiations at HIMAC, Japan have been performed within the HIMAC Research Projects: 11H282 and 14H282 "Ground based verifications of a European Crew Personal Active Dosimeter (EuCPAD) for Astronauts". We would like to thank Satoshi Kodaira, Hisashi Kitamura and Yukio Uchihori and the HIMAC operating team for their help and excellent support during the irradiation campaigns in Japan. We would also like to thank all colleagues from the various calibration labs SL, Austria; PTB, Germany; PSI, Switzerland, iThemba, South Africa for their help and support during the calibration runs.

We would like to thank all the astronauts and cosmonauts working with the EAD-system on-board the ISS especially Andreas Mogensen, Takuya Onishi and Thomas Pesquet. Further, we would like to thank the ESA USOCs (CADMOS, Toulouse, France and ECOS, Cologne, Germany) and our ESA Project Integration Manager (PIM), Lukas

Please cite this article as: U. Straube, T. Berger and M. Dieckmann, The ESA Active Dosimeter (EAD) system onboard the International Space Station (ISS), Z Med Phys, https://doi.org/10.1016/j.zemedi.2023.03.001

De Smet, for continuous and excellent support during the mission on-board the ISS. For the payload operational aspects, the EAD-team wishes to thank Andreas Schoen for his support to fly the EAD-system on these two missions in 2015 and 2016, to which the presented data correspond. John Nolan deserves grateful mentioning for his initiative on the Columbus Multi-Purpose Computer and Communication, without which the EAD-system could not have performed data- up and down links. Rene Demes contributions from the ESA side, on the ESA DOSIS 3D deserves grateful mentioning, as these systems provided an excellent data reference to the EAD- system. DOSIS-3D-DOSTEL are available at: http://swe.ssa.esa.int/human-space-flight.

This work on the EAD-system presented here could not have been performed without the additional support of ESA Astronauts, Christer Fuglesang, Thomas Reiter and Paolo Nespoli, who all together paved the way for ESA on initiating personal radiation instrumentation developments.

References

[1] Straube U, Berger T, Reitz G, Facius R, Fuglesang C, et al. Operational radiation protection for astronauts and cosmonauts and correlated activities of ESA Medical Operations. *Acta Astronaut* 2010;66:963–973. https://doi.org/10.1016/j.actaastro.2009.10.004.

[2] EuCPAD 2016, EuCPAD Acceptance Data Package (ADP) Version 2.0 (17 May 2016). ESA CONTRACT NO. 4200023059/09/NL/CP

[3] ESA, Dosimeter System Patent No: WO 2015/024591/A1 (2015)

[4] Moro D, Chiriotti S. EuTEPC: measurement in gamma and neutron fields. Rad Prot Dosim 2015;166:266–270. https://doi.org/10.1093/rpd/ncv154.

[5] Mirion Technology (RADOS) Radiation Detector *US Patent US 5739541* (1998)

[6] Mirion Technologies https://www.mirion.com/products/dosimetry-system

[7] Mirion Technologies https://www.mirion.com/products/instadose-wireless-dosimeter

[8] ICRP. 1990 Recommendations of the international commission on radiological protection. *ICRP Publication 60. Ann. ICRP, 21* (1–3), 1–201, 1991.

[9] Reitz G, Berger T, Bilski P, Facius R, Hajek M, et al. Astronaut's Organ Doses Inferred from Measurements in a Human Phantom Outside the International Space Station. Radiat Res 2009;171 (2):225–235. https://doi.org/10.1667/RR1559.1.

[10] Luszik-Bhadra M, Wendt W. Method and Device for determining the personal dose in mixed neutron/photon fields. *US Patent US7208743B2* (2007).

[11] Luszik-Bhadra M, Nakhostin M, Niita K, Nolte R. Electronic personal neutron dosemeters for energies up to 100 MeV: calculations using the PHITS code. Radiat Meas 2008;43:1044–1048. https://doi.org/10.1016/j.radmeas.2007.10.047.

[12] Luszik-Bhadra M, Beck P, Berger T, Jaksic A, Latocha M, et al. Response calculations for silicon-based direct-reading dosimeters for use at the international space station (ISS). Radiat Meas 2010;45 (10):1548–1552. https://doi.org/10.1016/j.radmeas.2010.08.026.

[13] Yasuda H. Responses of a direct ion storage dosimeter (DIS-1) to heavy charged particles. Radiat Res 2001;156:805–808.

[14] McIlwain CE. Coordinates for mapping the distribution of magnetically trapped particles. J Geophys Res 1961;66 (11):3681–3691. https://doi.org/10.1029/JZ066i011p03681.

[15] Smart DF, Shea MA. A review of geomagnetic cutoff rigidities for earth orbiting spacecraft. *Adv Space Res* 2005;36(10):2012–2020. https://doi.org/10.1016/j.asr.2004.09.015.

[16] Berger T, Matthiä D, Burmeister S, Zeitlin C, Rios R, et al. Long term variations of galactic cosmic radiation on board the International Space Station, on the Moon and on the surface of Mars. J Space Weather Space Clim 2020;10:34. https://doi.org/10.1051/swsc/2020028.

[17] Berger T, Burmeister S, Matthiä D, Przybyla B, Reitz G, et al. DOSIS & DOSIS 3D: radiation measurements with the DOSTEL instruments on board the Columbus Laboratory of the ISS in the years 2009–2016. J Space Weather Space Clim 2017;7:A8. https://doi.org/10.1051/swsc/2017005.

[18] Berger T, Matthiä D, Burmeister S, Rios R, Lee K, et al. The Solar Particle Event on 10 September 2017 as observed on-board the International Space Station (ISS). Space Weather 2018;16:1173–1189. https://doi.org/10.1029/2018SW001920.

[19] Berger T, Przybyla B, Matthiä D, Reitz G, Burmeister S, et al. DOSIS & DOSIS 3D: Long term dose monitoring on board the Columbus Laboratory of the International Space Station (ISS). J Space Weather Space Clim 2016;6:A39. https://doi.org/10.1051/swsc/2016034.

Please cite this article as: U. Straube, T. Berger and M. Dieckmann, The ESA Active Dosimeter (EAD) system onboard the International Space Station (ISS), Z Med Phys, https://doi.org/10.1016/j.zemedi.2023.03.001